https://doi.org/10.26219/heal.aueb.6224

ATHENS UNIVERSITY OF ECONOMIC AND BUSINESS

DEPARTMENT OF STATISTICS

EWMA Control Charts for monitoring Poisson Observations

Author:
Vakerli Maria

Supervisor:
Psarakis Stelios

M.Sc Thesis

Submitted to the Department of Statistics
of the Athens University of Economics and Business
in partial fulfilment of the requirements for
the degree of Master of Science in Statistics

Athens, Greece
June 2023

https://doi.org/10.26219/heal.aueb.6224

ΟΙΚΟΝΟΜΙΚΟ ΠΑΝΕΠΙΣΤΗΜΙΟ ΑΘΗΝΩΝ

ΤΜΗΜΑ ΣΤΑΤΙΣΤΙΚΗΣ

Διαγράμματα ελέγχου εκθετικά σταθμισμένου κινητού μέσου για την παρακολούθηση Poisson παρατηρήσεων

Συγγραφέας:
Βακερλή Μαρία

Επιβλέπων:
Ψαράκης Στέλιος

Μεταπτυχιακή Διατριβή
Που υποβλήθηκε στο Τμήμα Στατιστικής
του Οικονομικού Πανεπιστημίου Αθηνών
ως μέρος των απαιτήσεων για την απόκτηση
Μεταπτυχιακού Διπλώματος Ειδίκευσης στη Στατιστική

Αθήνα, Ελλάδα
Ιούνιος 2023

https://doi.org/10.26219/heal.aueb.6224

https://doi.org/10.26219/heal.aueb.6224

ACKNOWLEDGEMENTS

I would like to express my sincere appreciation to my supervisor Prof. Stelios Psarakis whose exceptional mentorship and guidance have been invaluable in the completion of this thesis. His vast knowledge, expertise and dedication to teaching have been a constant source of inspiration, and I feel privileged to have had the opportunity to learn from him.

I am also deeply grateful to my mother for her unwavering love, support, and sacrifices. She has been my role model and my biggest cheerleader, and her persistent belief in me has given me the strength and determination to overcome any challenge.

Lastly, I would like to extend my thanks to the rest of my family and friends for their consistent support, encouragement, and understanding. Your support has been indispensable to me and has made all the difference in my academic journey.

https://doi.org/10.26219/heal.aueb.6224

ABSTRACT

The necessity for advanced statistical approaches that efficiently monitor and detect abnormalities in diverse industrial and service processes has been pushed by the growing emphasis on quality control and process improvement. Exponentially Weighted Moving Average (EWMA) control charts, created specifically for Poisson observations, are the main topic of this Master's Thesis.

The main goal of this research is on understanding the fundamental principles of quality control, control charts, and their specific relevance to Poisson data. Poisson observations are frequently seen in fields where discrete count data, such as defect counts, customer complaints, or the incidence of unusual events, are prevalent.

A thorough literature assessment will be part of the research methodology to assess the body of knowledge already available on control charts, EWMA methods, and Poisson processes. This thesis provides a thorough investigation of the use of sophisticated EWMA control charts for Poisson processes, covering important topics including method choice, mean monitoring, sample size adaptation, distribution considerations, and a practical application. The R statistical program will be used to implement some of the suggested control charts, and their performance and efficiency will be assessed using simulated data sets that represent various process scenarios. Finally, the conclusions of this thesis and some comments about further research will be discussed.

 https://doi.org/10.26219/heal.aueb.6224

ΠΕΡΙΛΗΨΗ

Η ανάγκη για προηγμένες στατιστικές προσεγγίσεις που παρακολουθούν και ανιχνεύουν αποτελεσματικά τις ανωμαλίες σε διάφορες βιομηχανικές διαδικασίες και διαδικασίες παροχής υπηρεσιών έχει ωθηθεί από την αυξανόμενη έμφαση στον ποιοτικό έλεγχο και τη βελτίωση της διαδικασίας. Τα διαγράμματα ελέγχου εκθετικά σταθμισμένου κινητού μέσου όρου (EWMA), που δημιουργήθηκαν ειδικά για τις παρατηρήσεις Poisson, είναι το κύριο θέμα αυτής της Μεταπτυχιακής Διατριβής.

Ο κύριος στόχος αυτής της έρευνας είναι η κατανόηση των θεμελιωδών αρχών του ποιοτικού ελέγχου, των διαγραμμάτων ελέγχου και της συγκεκριμένης συνάφειάς τους με τα δεδομένα Poisson. Οι παρατηρήσεις Poisson εμφανίζονται συχνά σε πεδία όπου επικρατούν διακριτά δεδομένα καταμέτρησης, όπως πλήθος ελαττωμάτων, παράπονα πελατών ή η συχνότητα εμφάνισης ασυνήθιστων γεγονότων.

Μια διεξοδική βιβλιογραφική αξιολόγηση θα είναι μέρος της έρευνας για την αξιολόγηση του συνόλου των γνώσεων που είναι ήδη διαθέσιμες σε διαγράμματα ελέγχου, μεθόδους EWMA και διαδικασίες Poisson. Αυτή η διατριβή παρέχει μια ενδελεχή διερεύνηση της χρήσης εξελιγμένων διαγραμμάτων ελέγχου EWMA για τις διαδικασίες Poisson, καλύπτοντας σημαντικά θέματα όπως η επιλογή μεθόδου, η παρακολούθηση του μέσου όρου, η προσαρμογή του μεγέθους του δείγματος, σκέψεις για την κατανομή και μια πρακτική εφαρμογή. Το στατιστικό πρόγραμμα R θα χρησιμοποιηθεί για την εφαρμογή ορισμένων από τα προτεινόμενα διαγράμματα ελέγχου και η απόδοση και η αποτελεσματικότητά τους θα αξιολογηθούν χρησιμοποιώντας προσομοιωμένα σύνολα δεδομένων που αντιπροσωπεύουν διάφορα σενάρια διεργασιών. Τέλος, θα συζητηθούν τα συμπεράσματα της παρούσας διπλωματικής εργασίας και ορισμένα σχόλια για περαιτέρω έρευνα.

https://doi.org/10.26219/heal.aueb.6224

https://doi.org/10.26219/heal.aueb.6224

Contents

https://doi.org/10.26219/heal.aueb.6224

https://doi.org/10.26219/heal.aueb.6224

https://doi.org/10.26219/heal.aueb.6224

List of Tables

 https://doi.org/10.26219/heal.aueb.6224

https://doi.org/10.26219/heal.aueb.6224

List of Figures

Chapter 1

Introduction

Statistical Quality Control(SQC) is a critical component in ensuring the consistency, reliability and effectiveness of industrial operations. Organizations can proactively monitor and control process variances, pinpoint potential causes of flaws or deviations, and make wise decisions to raise the general level of product or service quality by using statistical techniques and tools.

The control chart is a fundamental tool in SQC. Control charts depict process data graphically across time, allowing professionals to differentiate between common cause and special cause changes. These charts are useful for recognizing shifts, trends, or out-of-the-ordinary patterns that may signal an out-of-control scenario. Control charts aid to process stability and fault reduction by permitting timely intervention and corrective actions.

The Exponentially Weighted Moving Average (EWMA) chart is a significant type of control chart. EWMA charts prioritize current observations while giving older data an exponentially diminishing weight, in contrast to conventional control charts that give equal weight to all data points. Due to their enhanced sensitivity to slight variations in the process mean, EWMA charts are particularly good at spotting minute alterations or early indications of deterioration.

The Poisson distribution has a vital role in Statistical Quality Control, especially when dealing with count or occurrence data. The Poisson distribution represents the likelihood of a specified number of events occurring within a given time or space interval. The focus is on understanding and managing unusual events or occurrences, and it is frequently used in a variety of industries including manufacturing, healthcare, telecommunications, and finance.

The combination of EWMA control charts and Poisson data is a customized technique to monitoring operations regulated by the Poisson distribution. These specialized control charts provide an efficient method of identifying shifts and deviations in Poisson processes by combining the sensitivity and adaptability of EWMA charts with the distinctive properties of count data, including the discrete and non-negative nature of observations, independence assumptions, and the mean-variance relationship of the Poisson distribution. This integration improves the general quality and effectiveness of industrial systems by enabling practitioners to precisely monitor and enhance operations that are defined by uncommon events or occurrences.

https://doi.org/10.26219/heal.aueb.6224

Chapter 2

Control Charts: An overview

One of the fundamental tools for statistical process control is the control chart. Control charts are a type of graph used in production control to assess the stability of the control over the processes. The status is displayed on a graph, and the presence of data that deviates from the control limit lines or the usual trend is used to determine the occurrence of irregularities and when adjustments to the inputs should be done to return it to an under control state. In this chapter, fundamental characteristics and forms of control charts will be introduced.

2.1 Phases of Statistical Quality Control

The use of control charts, which serve as an important instrument in monitoring and managing processes, connects Phases I and II of Statistical Quality Control.

Effective SQC implementation starts with Phase I, Process Characterization. To fully comprehend the process and its underlying characteristics, data is gathered and analyzed during this phase. Establishing a baseline understanding of the process and locating potential sources of variance or quality problems are the main goals of Phase I. Numerous statistical methods are used, such as data analysis, study of the capability of the process, and identification of variance sources.

Phase II, Process Monitoring and Control, commences once Phase I is completed. To evaluate the process's performance over time, this phase mainly relies on control charts. The data collected and processed during Phase I is used to determine control limits on the charts, such as process mean and variation. Typically, control limits are established on a given number of standard deviations from the process mean or range.

During Phase II, information is persistently collected from the method and plotted on the control charts. The charts enable professionals to screen the method and distinguish signals of uncommon cause variety. These signals may incorporate information focuses falling exterior the control limits, particular designs, or runs. When a signal is identified, it shows that the method is showing unordinary behavior that requires examination. This examination ordinarily includes recognizing the potential causes of the variety and executing fitting remedial activities to bring the method back into control.

The connection between the two phases is critical. The knowledge acquired during Phase I serves as the foundation for choosing and putting control charts into use during Phase II. Phase I's knowledge of the procedure informs decisions like selecting the type of control chart and establishing control limits. Professionals can efficiently

https://doi.org/10.26219/heal.aueb.6224

monitor the process and promptly spot any deviations from the defined baseline thanks to control charts.

Overall, Phase I analysis is utilized to assess the unknown parameters of the method whereas Phase II centers on the observing of handle utilizing assessed control limits from Phase I investigation. These two phases work together to help firms develop a robust quality control framework and promote continuous improvement in processes.

2.2 Basic Principles of a Control Chart

Typically, in order to construct a control chart, we need control limits that will indicate whether or not the process is in control. The control limits are consisted of an upper control limit (UCL), a center line which indicates the average value of the quality attribute associated with the in-control condition (CL) and a lower control limit (LCL).

A point plotting within the control limits indicates that the process is in control. That implies, that if $Z_i \geq LCL \text{ and } Z_i \leq UCL$ the process is in control where Z_i is the observation at time *i*. Figure 2.1 depicts the appearance of a control chart when the process is in control.

Figure 2.1: Control chart when the process is in-control

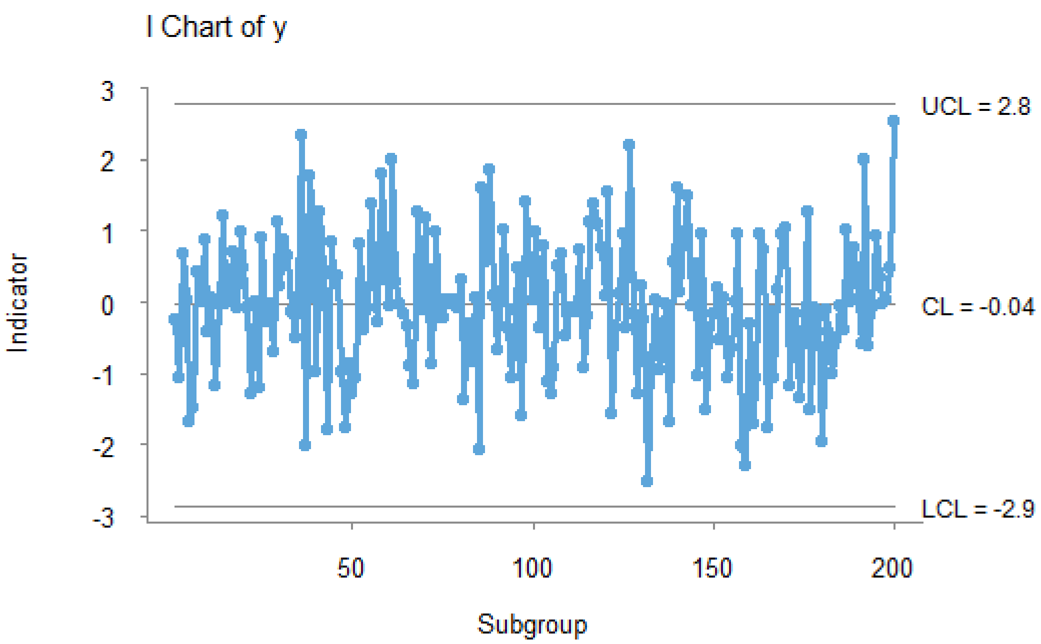

On the other hand, a point plotting outside the control limits indicates that the process probably is out of control. If $Z_i < LCL \text{ or } Z_i > UCL$ the process is out of control. These 2 options are represented optically in Figures 2.2 and 2.3 respectively.

Figure 2.2: Control chart when an observation is lower than the Lower Control Limit

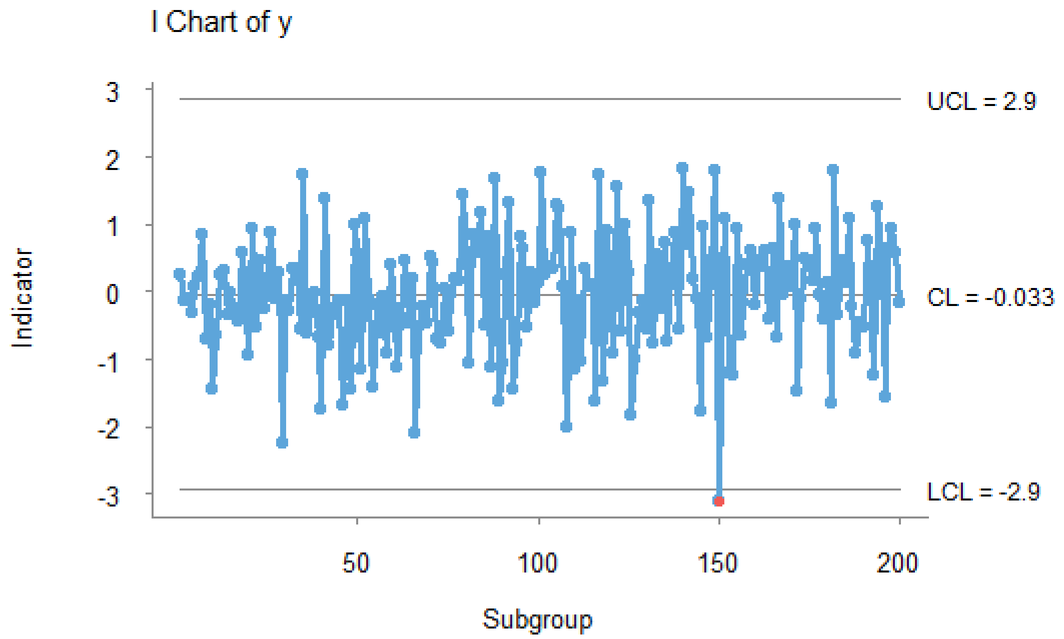

Figure 2.3: Control chart when an observation is greater than the Upper Control Limit

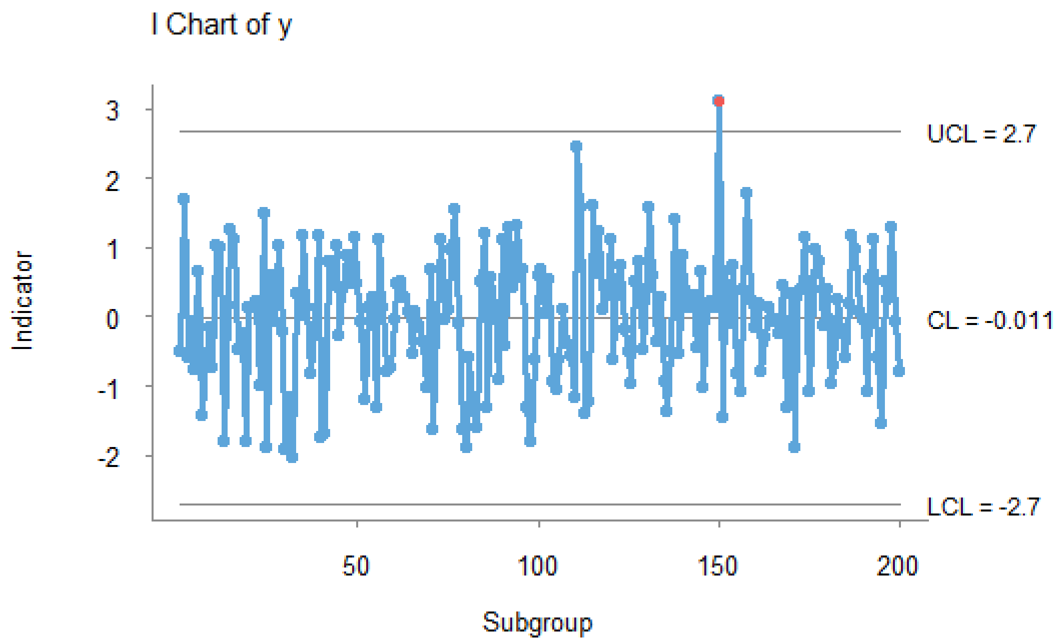

These are the common control charts that we use, when evaluating whether the process mean has increased or decreased and called two-sided control charts.

In very many cases, we are only concerned with the process mean increasing or decreasing, not both. Therefore, we use the one-sided control charts.

If we wish to see if the process mean has decreased, we use a lower-sided control chart and look for any points that are lower than the Lower Control Limit. The Upper

https://doi.org/10.26219/heal.aueb.6224

Control Limit can be set to A which is an appropriate upper cut point chosen to keep the control chart from reaching to infinity. When the observation Z_i exceeds A, the Z_i is set to A.

If we want to recognize if the process mean has risen, we use an upper-sided control chart and search for any points that are greater than the Upper Control Limit. In this case, using the same logic as before, we set usually the Lower Control Limit to 0. When the observation Z_i is below 0, the Z_i is set to 0.

2.3 Types of Control Charts

2.3.1 Shewhart's Control Charts

Shewhart W. A.(1924) , proposed a general model for creating these control limits. Let Z represent the quality characteristic of interest, μ_z is the mean of Z and σ_z is the standard deviation of Z.

Then, the control limits are:

$$UCL = \mu_z + L\sigma_z \tag{2.1}$$

$$Center\ Line = \mu_z$$

$$LCL = \mu_z - L\sigma_z$$

where L is usually 3 due to the three-sigma control limits.

This compromise for L arise from the 68–95–99.7 rule. This means that the probability of falling in this area is 99.73% within these six deviations.

These control charts, which are created using these assumptions, are called Shewhart's control charts.

Generally, there are two forms of Shewhart's variable control charts, charts for data gathered in subgroups and charts for individual measures. The points in sub-grouped data reflect a subgroup statistic, such as the mean, range, or standard deviation. The points in individual measurements might be either individual observations or a statistic, like the moving range between two observations.

Qualitative data that can be recorded as an attribute are called attribute data. Examples include the quantity of flaws, the quantity of errors in a document, the quantity of items in a sample that are rejected, and the existence of paint imperfections. With the use of the p-, np-, c-, and u-charts, attribute data are evaluated.

Although Shewhart's control chart is a very powerful tool in Phase I of Statistical Process Control, a significant drawback is the fact that this type of control chart only considers the information about the process provided by the last sample observation

 https://doi.org/10.26219/heal.aueb.6224

and ignores any information provided by the complete series of points. Because of this property, minor process changes have little effect on the Shewhart's control chart. These control charts may be less useful in Phase II monitoring problems due to the process's tendency to operate under control, the availability of accurate estimates of process parameters (such as the mean and standard deviation), and the fact that assignable causes typically do not result in significant process upsets or disturbances.

The cumulative sum (CUSUM) control chart and the exponentially weighted moving average (EWMA) control chart are two highly effective alternatives to the Shewhart's control chart that can be utilized when tiny process alterations are of interest.

2.3.2 Cumulative Sum Control Charts (CUSUM)

Page E.S.(1954) suggested a more advanced technique than Shewhart in order to identify a small magnitude of the shift while using all of the previous observations.

The CUSUM chart displays the cumulative sums of the sample values' deviations from a target value.

Assume that samples of size $n \geq 1$ are collected, and that $\bar{x}_j$ is the average of the jth sample. If μ_0 is the process mean target, then the cumulative sum control chart is created by plotting the C_i statistic which is based on the process's current and previous data values such as :

$$C_i = \sum_{j=1}^{i} (\bar{x}_j - \mu_0) \tag{2.2}$$

where C_i is an abbreviation for the cumulative sum up to and including the *i-th* sample.

When the sample size is *n=1* then, $\bar{x} = x_i$ in the *i*th sample. As a result, the CUSUM recursion (2.2) becomes:

$$C_i = \sum_{j=1}^{i} (\bar{x}_j - \mu_0) = \ (x_i - \mu_0) + \sum_{j=1}^{i-1} (x_j - \mu_0) = (x_i - \mu_0) + C_{i-1} \tag{2.3}$$

We must also mention that the CUSUM's starting value, C_0, is assumed to be zero.

The cumulative sum defined in equation (2.2) is a random walk with mean zero if the process remains in control at the target value μ_0. If a common pattern develops in the plotted points, either upward or downward, we should take this as evidence that the process mean has shifted, and we should look for an assignable cause.

 https://doi.org/10.26219/heal.aueb.6224

Statistical control limits are prerequisite in order to construct a control chart. The tabular (or algorithmic) CUSUM and the CUSUM's V-mask form are the two ways that CUSUMs can be represented. The tabular CUSUM is preferred above the other two formats.

By aggregating derivations from μ_0 that are above target with one statistic C^+, the tabular cusum operates, and combining below-target derivations from m0 with another statistic C^-. One-sided upper and lower CUSUMs are the names given to the statistics C^+ and C^-, respectively, and this is how they are calculated:

$$C_i^{+} = \max\left[0, x_i - (\mu_0 + K) + C_{i-1}^{+}\right] \tag{2.4}$$

$$C_i^{-} = \max\left[0, (\mu_0 - K) - x_i + C_{i-1}^{-}\right]$$

where the starting values are $C_0^{+} = C_0^{-} = 0$

We must also mention that *K* is called the slack value or reference value. It is frequently chosen so that it is approximately halfway between the target μ_0 and the easily detectable out-of-control value of the mean μ_1.That means:

$$K = \frac{|\mu_1 - \mu_0|}{2} \tag{2.5}$$

The process is deemed to be out of control if either C_i^{+}or C_i^{-}surpass the decision interval *H*.

The best choice of these two parameters, *K* and *H*, is actually crucial because it significantly affects the CUSUM's performance. It is typically advised to choose these parameters to offer acceptable average run length performance. Some general advice for choosing *H* and *K* are based on these findings.

We define $H = h\sigma$ and $K = k\sigma$, where σ is the sample variable's standard deviation used to create the CUSUM. In general, a CUSUM with strong qualities against a shift of around *1σ* in the process mean can be obtained by using $h = 4$ or $h = 5$ and $k = \frac{1}{2}$.

2.3.3 Exponentially Weighted Moving Average Control Charts (EWMA)

Roberts S.W.(1952) introduced the Exponentially Weighted Moving Average (EWMA) control chart. EWMA is a statistic for tracking the process of averaging data in a method that devalues data as they become further out in time.

The standard recursion for EWMA is defined by:

https://doi.org/10.26219/heal.aueb.6224

$$Z_i = \lambda \cdot X_i + (1-\lambda) \cdot Z_{i-1} \; for \; i = 1,2.. \tag{2.6}$$

$$Z_0 = \mu_0$$

where:

Z_i is EWMA statistic at time *i*

μ_0 is starting value or target value (occasionally, the mean of historical data is used)

X_i is the collected statistic at time *i*

λ is a weighting parameter (also known as smoothing parameter), which takes values in (0,1] and determines the depth of memory of EWMA

The selection of the value λ must be done with the proper attention. A small value that is close to zero in an EWMA raises one potential issue. When the EWMA value is on one side of the center line, it may take the EWMA many periods to respond to a change in the mean because the small l does not give the new data much weight. This is being brought on by the inertia effect. The EWMA may find it more challenging to identify shifts as a result. If is set to a large value that is close to 1, it could take more time to detect a tiny shift. According to Montgomery (2009), the range [0.05,0.25] would be the best option for. Doing the calculations we have the following sequence:

$$Z_i = \lambda \cdot \sum_{j=0}^{i-1} (1-\lambda)^j \cdot X_i + (1-\lambda)^i \cdot Z_{i-1} \tag{2.7}$$

One must note that Shewhart's is a special case of EWMA if λ is set to 1.

If X_i are independent random variables with common variance σ^2, the variance of Z_i is:

$$\sigma_{Z_i}^2 = Var(Z_i) = \frac{\lambda}{2-\lambda}\left[1-(1-\lambda)^{2i}\right]\sigma^2 \tag{2.8}$$

The upper and lower control limits based on (2.1) are:

$$UCL = \mu_0 + L\sigma\sqrt{\frac{\lambda}{2-\lambda}[1-(1-\lambda)^{2i}]} \tag{2.9}$$

$$Center\ Line = \mu_0$$

https://doi.org/10.26219/heal.aueb.6224

$$LCL = \mu_0 - L\sigma\sqrt{\frac{\lambda}{2-\lambda}[1-(1-\lambda)^{2i}]}$$

which are also called time-varying control limits.

After running the EWMA for several samples *i* increases.

In consequence,

$$\lim_{i\to\infty}\frac{\lambda}{2-\lambda}\left[1-(1-\lambda)^{2i}\right] = \frac{\lambda}{2-\lambda} \quad (2.10)$$

Then, the control limits approach the steady-state values (also called asymptotic control limits) and Equation (2.9) takes the form:

$$UCL = \mu_0 + L\sigma\sqrt{\frac{\lambda}{2-\lambda}} \quad (2.11)$$

$$Center\ Line = \mu_0$$

$$LCL = \mu_0 - L\sigma\sqrt{\frac{\lambda}{2-\lambda}}$$

2.4 Hypothesis Testing

We must also recognize the close connection between control charts and hypothesis testing.

If the process is in control then process mean is μ_0. In the out of control case, process mean is not equal to μ_0.

It can be written equivalently as:

$$H_0 : \mu = \mu_0 \quad (2.12)$$

$$H_1 : \mu \neq \mu_0$$

for the two-tailed hypothesis testing and

$$H_0 : \mu = \mu_0 \quad (2.13)$$

$$H_1 : \mu > \mu_0$$

and

https://doi.org/10.26219/heal.aueb.6224

$$H_0 : \mu = \mu_0 \tag{2.14}$$

$$H_1 : \mu < \mu_0$$

for the one-tailed hypothesis testing.

We use a two-sided control chart in (2.12), an upper-sided control chart in (2.13), and a lower-sided control chart in (2.14).

Any choice based on a hypothesis test may not be the right one. There are two types of errors within the framework of hypothesis tests: type I error and type II error. A "false positive" error is when a genuine null hypothesis is rejected, whereas a "false negative" error is when a false null hypothesis is not rejected. To put it another way, a type I error involves spotting an effect that isn't there, but a type II error involves missing an effect that is.

In mathematical terms,

$$\begin{aligned} \alpha = Type\ I\ error &= \Pr(reject\ H_0 \mid \ H_0\ is\ true) \\ &= \Pr(signal\ out\ of\ control \mid the\ process\ is\ in\ control\ ) \\ &= \Pr(\mu \neq \mu_0 \mid \mu = \mu_0\ ) \end{aligned} \tag{2.15}$$

$$\begin{aligned} \beta = Type\ II\ error &= \Pr(fail\ to\ reject\ \ H_0 \mid \ H_1\ is\ true) \\ &= \Pr(does\ not\ signal \mid the\ process\ is\ out\ of\ control) \\ &= \Pr(\mu = \mu_0 \mid \mu = \mu_1\ ) \end{aligned} \tag{2.16}$$

where μ_0 is the in-control process mean and μ_1 is the out of control process mean.

There are four situations summarized in Table 2.1.

Table 2.1: Confusion Matrix of Hypothesis testing

	Reject H_0	**Fail to Reject H_0**
H_0 is true	*α*	*1-α*
H_1 is true	*1-β*	*β*

 https://doi.org/10.26219/heal.aueb.6224

2.5 The Poisson Distribution

The Poisson distribution is a discrete probability distribution that can be used to predict or explain the number of events that occur within a given time or space interval.

Let X be a random variable following a Poisson distribution, with parameter μ. Then, the probability mass function is:

$$\mathrm{P}(X = x) = \frac{e^{-\mu}\mu^x}{x!}, \qquad \mu > 0 \ \ and \ x = 0,1,2 \ldots \tag{2.17}$$

where:

x is the number of times an event occurs

e is the Euler's constant

μ is the average time an event occurs per interval

The positive real number μ is equal to the expected value of X and also its variance.

From a mathematical perspective,

$$E(X) = Var(X) = \mu \tag{2.18}$$

If the following presumptions are true, the Poisson distribution is a suitable model:

- x can have values of 0, 1, 2,..., and represents how many times an event happens in an interval.
- The likelihood that a second event will take place is unaffected by the occurrence of the first event. In other words, things happen on their own.
- The average rate of occurrences is unaffected by any occurrences. This is typically believed to remain constant for simplicity, although in reality, it may change over time.
- Only one event can take place at any given very small sub-interval; no other events can take place at that precise moment.

The Poisson Distribution is asymmetric, which means that it is always positively skewed, because it is inhibited on the left by the zero occurrence barrier and unlimited on the other side. As we can see in Figure 2.4, as long as μ increases, the graph looks more like a normal distribution.

https://doi.org/10.26219/heal.aueb.6224

Figure 2.4: Poisson Distribution when μ=5,10 and 20

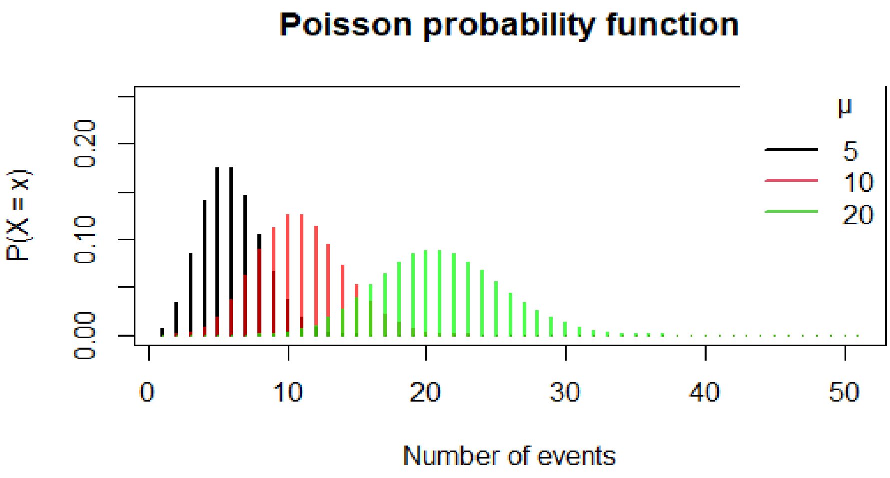

Poisson is one of the most used distributions in Statistical Quality Control since it can be employed to model the quality features, which may take the form of attribute counts. It is frequently implied as a model for the amount of flaws or nonconformities that exist in a single unit of product.

Let X be the number of nonconformities in a process. Then X follows Poisson distribution with probability mass function such as in (2.17).

Due to the fact that the observations X_1,X_2... are independent and identically distributed Poisson random variables with mean equals to μ_0 and variance equals to σ=$\sqrt{\mu_0}$, when process is in-control, (2.11) can take the form of:

$$UCL = \mu_0 + L\mu_0\sqrt{\frac{\lambda}{2-\lambda}} \tag{2.19}$$

$$Center\ Line = \mu_0$$

$$LCL = \mu_0 - L\mu_0\sqrt{\frac{\lambda}{2-\lambda}}$$

The Poisson distribution accurately models the presence of nonconformities in a sample. The c-chart and u-chart are two types of controls derived from the Shewhart's control chart and are used to monitor Poisson counts. The primary disparity observed between the aforementioned charts pertains to the nature of the data being subjected to plotting:

The c-chart is employed in situations where the process in question maintains a constant sample size, whereas the u-chart is utilized in cases where the sample size may differ across samples.

 https://doi.org/10.26219/heal.aueb.6224

2.5.1 c-chart

A c-chart is a type of control chart used to track the overall amount of nonconformities when analyzing subgroups from a process on a regular basis.

The total number of nonconformities in a subgroup is represented by each point on the graph. The average number of nonconformities is the middle line. The process average number of nonconformities per unit, if not otherwise stated, is calculated by dividing the total number of nonconformities by the sum of the subgroup sizes. Keep in mind that when the subgroup sizes are uneven, the center line changes.

The Poisson distribution has been assumed. That is, while there should be a low likelihood of finding nonconformity during an inspection, many nonconformities should theoretically be feasible, and the size of an inspection unit should remain constant over time. The normal approximation to the Poisson distribution is typically thought to be sufficient when k-sigma limits are applied, which typically needs the average number of nonconformities to be at least 5.

Let *c* be the number the overall amount of nonconformities in an inspection unit.

The control limits in c-chart are defined as:

$$UCL = \bar{c} + 3\sqrt{\bar{c}} \tag{2.20}$$

$$Center\ Line = \bar{c}$$

$$LCL = \bar{c} - 3\sqrt{\bar{c}}$$

where

$\bar{c}$ is an estimator representing the observed average number of nonconformities in a sample of inspection units.

If the results of these calculations are negative, we set the *LCL* equal to 0.

When the number of units in each subgroup is constant, a c-chart is advantageous since it is simpler to comprehend than a u-chart. The center line and control limits differ for data with varying subgroup sizes, making interpretation challenging. We should use a u-chart in this situation, which has variable control limits but a constant center line.

2.5.2 u-chart

The u-chart is a quality control chart that tracks the overall number of flaws per unit in various samples of size n; it makes the assumption that a unit may have multiple defects.

 https://doi.org/10.26219/heal.aueb.6224

It is a scaled-down variant of the c-chart known, which shows the average number of nonconformities per unit as opposed to the total number of nonconformities as c-chart. The same presumptions and advice are applicable.

The center line remains constant even though the control limits change for data with varied subgroup sizes. The points are plotted in units of standard deviation on a standardized control chart. Such a control chart makes it simpler to spot patterns by having a continuous center line at 0, as well as upper and lower control limits of -3 and +3.

We define as u the average number of nonconformities per inspection unit. That means that if a sample of *n* inspection units contains *x* total nonconformities, the average number of nonconformities per inspection unit is:

$$u = \frac{x}{n} \tag{2.21}$$

The control limits in u-chart are defined as:

$$UCL = \bar{u} + 3\sqrt{\frac{\bar{u}}{n}} \tag{2.22}$$

$$Center\ Line = \bar{u}$$

$$LCL = \bar{u} - 3\sqrt{\frac{\bar{u}}{n}}$$

where

$\bar{u}$ is the observed average number of nonconformities per unit in an initial set of data

2.6 Performance evaluation measures

In order to determine the performance of the control charts ARL (Average Run Length) is the main measure of effectiveness, along with others.

Run Length (*RL*) is the total number of samples collected before a signal is detected. Run length is a random variable with an integer range of values only. So, performance must be evaluated using the predicted value. The expected value of the run length, or the anticipated number of subgroups up until a control chart first signals, is known as *ARL* (Average Run Length).

There are two types of *ARL* that are described in literature:

https://doi.org/10.26219/heal.aueb.6224

ARL_0 or in-control ARL is the expected number of samples before a control chart signals while the process is in control. It is also known as false alarm.

ARL_1 or out-of-control ARL is the expected number of samples before a control chart signals while the process is out control.

The best control chart will obviously be the one with the biggest ARL_0 and smallest ARL_1. Unfortunately, this cannot be accomplished at the same time.

In case of uncorrelated observations, such as Shewhart's, the *ARLs* can be computed using (2.15) and (2.16):

$$ARL_0 = E(RL) = \sum_{k=1}^{\infty} k(1-\alpha)^{k-1} a = \frac{1}{a} \tag{2.23}$$

$$ARL_1 = E(RL) = \sum_{k=1}^{\infty} k\beta^{k-1}(1-\beta) = \frac{1}{1-\beta} \tag{2.24}$$

where *k* is the number of samples taken before an out of control signal occurs.

To have the biggest ARL_0 and smallest ARL_1, both types of errors must be controlled and minimized simultaneously. They are, however, mutually exclusive. You cannot reject and fail to reject the null hypothesis at the same time. It has to be either one or the other.

Comparable to the ARL, the SDRL is a metric utilized to assess the efficacy of a control chart in identifying alterations in the course of a process. However, the SDRL primarily concentrates on identifying modifications in the standard deviation of the process, as opposed to changes in the process mean. The statistical measure known as the standard deviation run length (SDRL) denotes the mean number of observations that a control chart necessitates in order to detect a change in the process standard deviation, deviating from the desired threshold value.

The use of SDRL is a crucial methodology within the context of Statistical Quality Control due to its potential to reveal how alterations in the process standard deviation may impact product quality distinctively from modifications affecting the process mean. Changes in the standard deviation may give rise to augmented variability in the output of the product, thereby giving rise to the production of items that fail to conform to the specifications demanded by customers. Consequently, the utilization of a control chart to monitor the process standard deviation can be deemed as a tool to uphold product quality within the acceptable bounds.

https://doi.org/10.26219/heal.aueb.6224

To summarize, both Average Run Length (ARL) and Standard Deviation Run Length (SDRL) are statistical metrics implemented in Statistical Quality Control (SQC) to assess the effectiveness of a control chart. The assessment of a control chart's efficacy in detecting alterations in process mean is achieved through utilization of the Average Run Length (ARL), whereas evaluation of its ability to detect changes in process standard deviation is accomplished through employment of the Standard Deviation Run Length (SDRL).

 https://doi.org/10.26219/heal.aueb.6224

Chapter 3

EWMA control charts for monitoring mean in Poisson processes

Throughout the years, numerous researchers have attempted to enhance the existing Exponential Weighted Moving Average (EWMA) control chart, first proposed by Roberts (1952) , in order to make it more effective at detecting shifts in the mean of a process more rapidly. Especially for the Poisson distribution, which is typically used to track how many nonconformities or flaws there are in a unit as a result of a repeating operation, significant work has been done.

Since independent and identically distributed Poisson random variables are typically used to describe the counts of events collected at regular intervals, detecting a change in an event's rate of occurrence can be thought of as detecting a change in the Poisson mean. In this chapter, some modifications of EWMA control chart are introduced to monitor Poisson process mean.

3.1 Ceiling, Round and Floor Exponentially Weighted Moving Average Control Chart

Given that EWMA control charts can be used both for measurement data and attribute data in case of count processes , such as Poisson, they have a significant disadvantage. They do not maintain the distinct range of possible values Z_i.

For this reason, Gan(1990a) proposed three modified exponentially weighted moving averages(EWMA) control charts for Poisson observations in which he used a method to convert the EWMA statistic to an integer value in order to preserve the discrete range.

As a reminder, the standard recursion for EWMA is defined by:

$$Z_i = \lambda \cdot X_i + (1-\lambda) \cdot Z_{i-1} \; for \; i = 1,2.. \tag{3.1}$$

$$Z_0 = \mu_0$$

where:

Z_i is EWMA statistic at time *i*

μ_0 is starting value or target value (occasionally, the mean of historical data is used)

https://doi.org/10.26219/heal.aueb.6224

X_i is the collected statistic at time i

λ is a weighting parameter (also known as smoothing parameter), which takes values in (0,1] and determines the depth of memory of EWMA

The three new modified EWMA statistics are the following:

$$Z_i = Ceil(\lambda \cdot X_i + (1-\lambda) \cdot Z_{i-1}) \tag{3.2}$$

$$Z_i = Round(\lambda \cdot X_i + (1-\lambda) \cdot Z_{i-1}) \tag{3.3}$$

$$Z_i = Floor(\lambda \cdot X_i + (1-\lambda) \cdot Z_{i-1}) \tag{3.4}$$

$$Z_0 = \mu_0$$

$$for\ i = 1,2..$$

where Ceil(x) indicates the smallest integer greater than or equal to x, Round(x) indicates that x is rounded to the nearest integer and Floor(x) indicates the largest integer less than or equal to x.

These modifications are titled as CEWMA, REWMA and FEWMA respectively.

Each one of them was designed for a specific reason:

- The purpose of the CEWMA control chart is to allow the EWMA to accumulate modest increases faster on the upper side.
- The FEWMA control chart is made to help the EWMA accumulate modest decreases to the bottom side more quickly.
- The REWMA control chart is roughly equivalent to the unmodified EWMA

Thereinafter, he compares the new control charts with Shewhart's, in terms of ARL_1, in order to conclude which is more effective in detecting shifts in the process mean. The comparison involved one-sided EWMAs with one-sided Shewhart's (both upper and lower) and two-sided EWMA with two-sided Shewhart's control chart.

We must emphasize that he did not employ any of the previously discussed control limits. His criterion for selecting the control limits, and thus the modified EWMA with the appropriate weighting parameter λ, was that the ARL_0 should be greater or nearly equal to Shewhart's.

We must also mention that, in all 3 tables, μ represents the process mean. When the process mean μ is equal to the in-control process mean ,provided each time, the corresponding results in this line are the ARL_0 .

Some of the results of the comparison of the ARL of upper-sided Shewhart's and upper modified EWMAs can be shown in Table 3.1.

https://doi.org/10.26219/heal.aueb.6224

Only if the process mean has increased are we interested in the upper case. The criterion we previously discussed led to the selection of the upper control limit. Contrarily, the lower control limit is set to zero, indicating that these control charts will never issue an out-of-control signal since for all practical purposes. Therefore, if $Z_i > UCL$, we get an out-of-control signal.

Table 3.1: Comparison of Upper-Sided Shewhart's Average Run Length and Upper-Sided modified EWMA's Average Run Length when the process mean μ_0 is 12

μ	Shewhart λ=1	CEWMA λ=0.769	CEWMA λ=0.77	CEWMA λ=0.5	REWMA λ=0.5	CEWMA λ=0.3	FEWMA λ=0.3
12	1458.5	1583.9	1457.1	1464.2	1464.2	1569.2	1561.3
13	501.4	444.2	419.3	301.5	301.5	227.6	$\boxed{223.0}$
18	14.7	9.7	9.5	6.3	6.3	6.1	$\boxed{4.8}$
25	1.9	1.8	1.7	1.8	1.8	2.3	$\boxed{1.7}$
30	1.2	1.2	1.2	1.3	1.3	1.7	$\boxed{1.2}$

From Table 3.1, all of the three modified control charts are more efficient from Shewhart's in small changes. In addition all control charts have a tendency to quickly identify significant shifts in favor of a higher value. Furthermore, as the smoothing parameter λ lowers, the upper-sided modified EWMA control charts get more better at spotting minor shifts towards a bigger value. It may be observed that with the same weighting parameter λ=0.5 CEWMA and REWMA give the exact same results. Overall, it could be seen easily that FEWMA (λ=0.30) has a superiority over the others control charts in the upper side case.

Table 3.2 displays some of the findings from the comparison of the lower-sided Shewhart and lower modified EWMAs' ARLs.

In lower case, we are interested only if the process mean has decreased. The criterion we previously stated resulted to the selection of the lower control limit. For the upper control limit we set a truncation point A equals to 30. Therefore, if $Z_i < LCL$, we get an out-of-control signal.

https://doi.org/10.26219/heal.aueb.6224

Table 3.2: Comparison of Lower-Sided Shewhart's Average Run Length and Lower-Sided modified EWMA's Average Run Length when the process mean μ_0 is 20

μ	Shewhart λ=1	CEWMA λ=0.4	REWMA λ=0.4	FEWMA λ=0.4	CEWMA λ=0.2	REWMA λ=0.2	FEWMA λ=0.2
5	$\boxed{1.2}$	1.4	1.7	1.9	1.4	2.1	2.7
6	$\boxed{1.3}$	1.6	1.9	2.0	1.6	2.2	2.9
7	$\boxed{1.7}$	1.8	2.0	2.1	$\boxed{1.7}$	2.4	3.1
13	18.5	4.8	5.1	5.3	$\boxed{3.9}$	5.4	6.5
19	660.8	325.7	326.7	327.4	$\boxed{244.6}$	252.7	256.1
20	1284.4	1228.7	1230.2	1231.1	1420.0	1435.6	1440.5

Table 3.2 shows us that, all of the three modified control charts are more efficient from Shewhart's in small changes. When the smoothing parameter λ lowers, the lower-sided modified EWMA control charts get more better at spotting minor shifts towards a smaller value. When EWMAs are compared using the same parameter, CEWMA is superior to the other two. Last but not least, it should be noted that although our results are comparable to those of all the control charts for larger changes, Shewhart's is marginally more accurate in identifying these kinds of shifts.

For the two sided case, control limits were chosen due to the criteria we mentioned before, and now we are interested in both an increase and a decrease in the process mean. When $Z_i < LCL \; or \; Z_i > UCL$, an out-of-control signal is generated.

Table 3.3 displays some of the comparison's observations.

Table 3.3: Comparison between Two-sided Modified Exponentially Weighted Moving Average control chart Average Run Lengths with Two-sided Shewhart's control chart when process mean μ_0 is 20

μ	Shewhart λ=1	CEWMA λ=0.9	FEWMA λ=0.82	REWMA λ=0.86	CEWMA λ=0.89	CEWMA λ=0.57	CEWMA λ=0.27

 https://doi.org/10.26219/heal.aueb.6224

6	3.5	4.0	$\boxed{1.8}$	2.3	4.0	2.6	3.7
11	66.2	74.9	$\boxed{8.8}$	22.1	80.0	13.2	11.2
19	2737.7	3114.2	$\boxed{1763.3}$	3052.2	3281.6	5105.4	8906.1
20	1218.6	1217.1	1219.5	1291.4	1259.6	1384.5	1234.5
21	551.0	513.4	548.1	534.3	525.3	435.2	$\boxed{257.9}$
26	27.5	22.3	20.4	21.1	22.4	12.1	$\boxed{8.4}$
30	6.4	5.4	4.9	5.1	5.4	$\boxed{3.9}$	$\boxed{4.0}$

Generally, we can see that if the smoothing parameter λ decreases, the modified EWMA control charts become more adept at spotting small shifts.

Especially, regarding the change of the process mean to a higher value, CEWMA with λ=0.27 is more effective than the others.

As far as it concerns the change of the process mean to a smaller value, it is obvious that FEWMA with λ=0.82 is superior to all the other control charts. However, we must note that in a small shift, Shewhart's ARL_1 is lower than most of the other control charts.

All of the modified EWMA control charts are better at spotting modest shifts in favor of larger values instead of lower values, and all control charts have a tendency to detect big shifts in favor of larger values rapidly.

Finally, the more efficient a two-sided modified EWMA control chart is at accurately detecting shifts to a higher value, the less efficient it becomes at detecting various shifts to a smaller value.

In conclusion, in order to employ the EWMA for attribute data due to the rounding to an integer, Gan introduced 3 modifications. The findings show that the FEWMA should be used if we are interested in whether the mean process has increased. The CEWMA control chart is the best choice if we're looking if the process mean has reduced. In general, the one-sided modified EWMA serve their goal.

In the case of the two sided control charts, the modified EWMA control charts are better at detecting tiny movements in the direction of a larger value. But, the two-sided Shewhart's control chart and the two-sided modified EWMA control charts both quickly detect significant shifts. A two-sided modified EWMA control chart becomes

https://doi.org/10.26219/heal.aueb.6224

less successful at detecting minor changes towards smaller values the better it is at detecting small shifts towards larger values. In this regard, the two-sided Shewhart's control chart performs better in the detection of tiny shifts towards a smaller value than the majority of the two-sided modified EWMA control charts taken into consideration in Table 3. His suggestion is to choose a two-sided modified EWMA control chart so that the in-control ARL is the largest when the process mean is at the in-control process mean in order to detect shifts close to the in-control process mean. This type of control chart is typically uniformly more effective than the two-sided Shewhart's control chart.

3.2 Poisson Exponentially Weighted Moving Average Control Chart

Although Gan proved the superiority of these three modified EWMA control charts over Shewhart's, some information is lost due to the rounding to an integer.

Borror et al.(1998) proposed the Poisson EWMA, denoted as PEWMA, for monitoring the Poisson data, where the exact value of the statistic is calculated and plotted in the chart as in (3.1).

As a reminder, as we previously discussed, if X_i are independent random variables with common variance σ^2 , the variance of Z_i is:

$$\sigma_{Z_i}^2 = Var(Z_i) = \frac{\lambda}{2-\lambda}\left[1-(1-\lambda)^{2i}\right]\sigma^2 \tag{3.5}$$

Therefore, time-varying control limits based on (3.5) are:

$$UCL_i = \mu_0 + L\sigma\sqrt{\frac{\lambda}{2-\lambda}[1-(1-\lambda)^{2i}]} \tag{3.6}$$

$$Center\ Line = \mu_0$$

$$LCL_i = \mu_0 - L\sigma\sqrt{\frac{\lambda}{2-\lambda}[1-(1-\lambda)^{2i}]}$$

As *i* increases, we do have:

$$\lim_{i\to\infty}\frac{\lambda}{2-\lambda}\left[1-(1-\lambda)^{2i}\right] = \frac{\lambda}{2-\lambda} \tag{3.7}$$

Then, the asymptotic control limits are:

$$UCL = \mu_0 + L\sigma\sqrt{\frac{\lambda}{2-\lambda}} \tag{3.8}$$

$$Center\ Line\ =\ \mu_0$$

$$LCL = \mu_0 - L\sigma\sqrt{\frac{\lambda}{2-\lambda}}$$

Due to the fact that the observations *X1,X2...* are independent and identically distributed Poisson random variables with mean equals to μ_0 and variance equals to σ=$\sqrt{\mu_0}$, the asymptotic control limits from 3.8 are:

$$UCL = \mu_0 + L\mu_0\sqrt{\frac{\lambda}{2-\lambda}} \tag{3.9}$$

$$Center\ Line\ =\ \mu_0$$

$$LCL = \mu_0 - L\mu_0\sqrt{\frac{\lambda}{2-\lambda}}$$

At this stage, it's vital to note that the Poisson distribution is skewed. Therefore, the application of symmetrical control limits will result in a control chart that is more effective at identifying shifts in the process mean in the direction of bigger values and less effective at identifying such shifts in the direction of smaller values. This is allowed if the identification of shifts towards a larger value is more important than the detection of shifts towards a smaller value. The use of symmetrical action limits is problematic if detecting shifts towards smaller values is more important than detecting movements towards larger values.

Using this as a trigger, the following are the new control limits they suggested be used when constructing the PEWMA:

$$UCL = \mu_0 - A_U\,\mu_0\sqrt{\frac{\lambda}{2-\lambda}} \tag{3.10}$$

$$Center\ Line\ =\ \mu_0$$

$$LCL = \mu_0 - A_L\mu_0\sqrt{\frac{\lambda}{2-\lambda}}$$

It is common practice to set the values of A_U and A_L to be equal ($A = A_U = A_L$), but there are situations when creating asymmetric control charts can be useful as we said before. The choice of the value A depends on the user in order to achieved the desired in-control ARL.

Due to the nonnegative nature of the EWMA statistic provided in equation 3.1, the EWMA chart will not indicate at a lower control limit that is less than or equal to

https://doi.org/10.26219/heal.aueb.6224

zero. As a result, we set *LCL*=0 if the computed value of LCL is less than zero. Assigning $A_U \neq A_L$ in this case might be helpful in ensuring that the lower control limit is nonzero and that a downward shift can be identified.

In Table 3.4, we can see the PEWMA, Gan's modifications and Shewhart's control charts which are compared in terms of ARL_1. We must refer that the value of *A* was selected so that the in-control ARL would resemble the ARLs provided by Gan(1990a) and all of the ARL_0*s* are greater than Shewhart's.

Table 3.4: Comparison of PEWMA, CEWMA, REWMA and Shewhart's control charts when in control mean is $\mu_0 = 20$

μ	Shewhart λ=1	REWMA λ=0.86	PEWMA λ=0.86	CEWMA λ=0.57	PEWMA λ=0.57	CEWMA λ=0.27	PEWMA λ=0.27
8	10.0	4.5	4.5	3.9	$\boxed{2.7}$	5.0	$\boxed{2.7}$
14	553.7	202.5	203.0	172.7	28.4	138.5	$\boxed{8.5}$
18	4876.2	4391.9	4380.6	14341.5	1486.3	89688.2	$\boxed{197.2}$
20	1218.6	1291.4	1291.8	1384.5	1383.7	1234.5	1233.4
22	266.1	238.8	238.5	160.9	168.7	$\boxed{78.8}$	85.2
26	27.5	21.1	21.1	12.1	12.3	8.4	$\boxed{7.8}$

When looking at the findings in Table 3.4, one can see that the more the weighting parameter λ decreases, the more efficient the control chart becomes in detecting shifts. This arises due to the fact that λ determines the rate at which older data enter into the calculation of the EWMA statistic. A small value of λ gives more weight to older data, allowing us to understand the change more quickly.

Additionally, in the comparison between the control charts with the same λ, PEWMA outperforms in almost all cases.

Lastly, for almost all shifts, PEWMA with λ=0.57 and λ=0.27 have smaller ARL_1 both from Shewhart's and Gan's modifications.

https://doi.org/10.26219/heal.aueb.6224

3.2.1 Estimated parameters on PEWMA control charts

Until here, we have supposed that the real in-control process mean μ_0 is known. However, the process's mean is often unknown.

When the process parameters are unknown, a strategy that is frequently utilized in these situations is to carry out a retrospective study, in which a reference sample of observations is acquired and then used to estimate these unknown characteristics.

Testik et al.(2006) studied the impact of estimated mean on the performance of Poisson EWMA control charts. The proposed chart's performance was assessed using RL features like ARL and SDRL. In this case, the run length distribution is determined by the estimated parameter values. This is why they used additional measures such as Standard Deviation of Run Length, noted as SDRL.

An estimator of μ_0 is used, denoted by $\widehat{\mu_0}$, has been used in place of μ_0 in 3.6 in order to create the control chart.

The maximum likelihood estimator for μ_0 is:

$$L(\mu_0; x_{1,\dots,}x_n) = \prod_{i=1}^{n} e^{-\mu_0}\, {\mu_0}^{x_i} \frac{1}{x_i!} \tag{3.11}$$

$$l(\mu_0; x_{1,\dots,}x_n) = \log\left(L\left(\mu_0; x_{1,\dots,}x_n\right)\right) = -n\mu_0 + \sum_{i=1}^{n} \ln\left(x_i!\right) + ln(\mu_0)\sum_{i=1}^{n} x_i \tag{3.12}$$

After calculating the derivative of the natural log likelihood function with respect to μ_0 , set it to zero and solve for μ_0, the equation is :

$$\widehat{\mu_0} = \frac{1}{n}\sum_{i=1}^{n} x_i \tag{3.13}$$

where *n* is the size of our reference sample.

From (3.10) and the use of (3.13) the new control limits are the following:

$$UCL = \widehat{\mu_0} + A_U\, \widehat{\mu_0}\sqrt{\frac{\lambda}{2-\lambda}} \tag{3.14}$$

$$Center\ Line = \widehat{\mu_0}$$

$$LCL = \widehat{\mu_0} - A_L\widehat{\mu_0}\sqrt{\frac{\lambda}{2-\lambda}}$$

However, if the parameters are not accurately estimated, the operational performance of a control chart may deviate dramatically from the expected performance. They have assumed that a reference sample of observations has been collected, the mean of the in control process has been estimated, and the Poisson EWMA control chart has

https://doi.org/10.26219/heal.aueb.6224

been built. The control chart's run length will follow some conditional distribution, which will be determined by the particular realization of the process mean estimate.

In order to normally provide performance that is relatively close to the known process mean chart, it is necessary to approximate which n would be more suitable as a reference sample because $\widehat{\mu_0}$ is an estimate of μ_0 and depends on n.

The Markov chain approach was used to assess the chart's conditional and marginal run length performance in terms of average run length and standard deviation of run length. The findings suggest that sample sizes bigger than 300 would typically produce performance that is quite near to the known process mean chart. When estimation is applied, the performance of the in-control average run length may be considerably affected.

3.3 Poisson Double Exponentially Weighted Moving Average Control Charts

Zhang et al.(2003) expand on the PEWMA chart's concept to produce a new chart that we refer to as a Poisson Double EWMA control chart, denoted as PDEWMA.

Let X be the number of nonconformities in a process.

Then, the observations X_1,X_2... are independent and identically distributed Poisson random variables with mean equals to μ and variance equals to μ.When the process is in control μ=μ_0.

Our Double EWMA control statistic, Y_i, is defined by the system of equations to track changes in the process mean:

$$Z_i = \lambda \cdot X_i + (1-\lambda) \cdot Z_{i-1} \; for \; i = 1{,}2.. \tag{3.15}$$

$$Z_0 = \mu_0$$

$$Y_i = \lambda \cdot Z_i + (1-\lambda) \cdot Y_{i-1} \; for \; i = 1{,}2..$$

$$Y_0 = \mu_0$$

where Z_i is the usual EWMA statistic and DEWMA statistic Y_i is an EWMA of Z_i.

Therefore,

$$Var(Y_i) = \frac{\lambda^4\left[1+(1-\lambda)^2-(i+1)^2(1-\lambda)^{2i}+\left(2i^2+2i-1\right)(1-\lambda)^{2i+2} - i^2\,(1-\lambda)^{2i+4}\right]}{[1-(1-\lambda)^2]^3} \tag{3.16}$$

where λ is ,as before, the weighting parameter and i the time.

https://doi.org/10.26219/heal.aueb.6224

The time-varying control limits are set now as:

$$UCL_i = \mu_0 + K\sqrt{Var(Y_i)} \tag{3.17}$$

$$Center\ Line = \mu_0$$

$$LCL_i = \mu_0 - K\sqrt{Var(Y_i)}$$

The performance of the PDEWMA chart is determined by the smoothing constant λ and the control limit constant $K > 0$ in this case.

To compare PDEWMA and PEWMA, we must also use time-varying control limits for the PEWMA, instead of the asymptotic, which are:

$$UCL_i = \mu_0 + L\sqrt{Var(Z_i)} \tag{3.18}$$

$$Center\ Line = \mu_0$$

$$LCL_i = \mu_0 - L\sqrt{Var(Z_i)}$$

We must remember that Z_i follows Poisson distribution. As a result, the mean and variance are equal, $\sigma=\sqrt{\mu}$ .Then we do have:

$$Var(Z_i)=\frac{\lambda}{2-\lambda}\left[1-(1-\lambda)^{2i}\right]\sigma^2 = \frac{\lambda}{2-\lambda}\left[1-(1-\lambda)^{2i}\right]\mu^2 \tag{3.19}$$

They employed ARLs and SDRLs as their measurements for the comparison of PEWMA and PDEWMA. In Table 3.5 we can see some of the results when the in-control process mean is μ_0 =8 with different λ values. We must also point out that the corresponding result in this line where μ=μ_0 =8 is the ARL_0 , and is 200 in both control charts, and also some SDRLs measures are provided.

Table 3.5: Comparison of PDEWMA and PEWMA in terms of ARL and SDRL when μ_0 =8

λ	μ	ARL		SDRL	
		PDEWMA	**PEWMA**	**PDEWMA**	**PEWMA**
0.05	6	$\boxed{8.1}$	10.2	7.0	6.9
	8	200.2	200.2	250.6	217.1
	9	$\boxed{24.5}$	27.9	24.7	25.2
0.25	6	$\boxed{12.5}$	18.7	9.0	14.6
	8	200.1	200.3	203.5	201.1

https://doi.org/10.26219/heal.aueb.6224

	9	$\boxed{36.5}$	40.2	34.8	38.0
0.5	6	$\boxed{22.3}$	57.4	19.4	54.8
	8	200.1	200.6	200.1	196.5
	9	$\boxed{44.9}$	50.4	43.5	49.8

The findings, in Table 3.5, show that all the ARLs of PDEWMA are smaller than of PEWMA, all the SDRLs of PEWMA are greater than or roughly same to those of PDEWMA except from the in-control SDRL when λ=0.05 where we have a great difference in favor of PDEWMA. Furthermore, a lower value of λ makes both charts more responsive to the shifts in the process mean because ARL_1 shrinks as decreases. A very small λ, on the other hand, indicates a larger in-control SDRL.

One may observe that this is a concern about that because if the EWMA value is on one side of the center line while the mean changes in the opposite direction occurs, the EWMA may take several periods to react to the change because the small λ gives more weight to the older data. This is known as the inertia effect. It has the potential to reduce the EWMA's effectiveness in shift detection.

As a conclusion, the PDEWMA chart outperforms the PEWMA chart in detecting small process mean decreases and performs similarly to or slightly better than the PEWMA chart in detecting large process mean shifts. In conclusion, the PDEWMA chart outperforms the PEWMA chart.

3.4 Two-out-of-two(2/2) runs rule with Fast Initial Response PEWMA control chart

Afterward, Abujiya et al.(2013) , proposed the application of fast initial response (FIR) using $2/2$ runs rule scheme for monitoring Poisson observations to improve the sensitivity of the existing PEWMA and PDEWMA control charts. Up to this point, the runs rules were only applicable to Shewhart-type control charts. Their purpose was to prove that the use of the runs rule and the FIR feature significantly increase the sensitivity of the Poisson EWMA control chart while decreasing the out-of-control ARL.

Fast Initial Response(FIR) or headstart was first devised by Lucas and Crosier (1982) for the CUSUM contol charts. FIR sets the starting value to a non zero value. The procedure's benefit would be its ability to more immediately detect a process that isn't on target when it starts.(Montgomery,2009)

https://doi.org/10.26219/heal.aueb.6224

Some methods have been proposed to the extension to EWMA. For example, two one-sided EWMA charts were created by Rhoads et al. (1996) and are initially set at values halfway between the target and the control limit.

where F_{adj} stands for FIR feature:

$$F_{adj} = 1 - (1 - f)^{1+a(i-1)} \tag{3.20}$$

a>0 is an adjustment parameter and *f* the distance from the target value with 0 < *f* ≤1.

To guarantee that the long-term run length properties of the EWMA chart would be essentially unaffected, the influence of the FIR adjustment diminishes over time. According to Steiner S.H.(1999), the initial time period's time-varying bounds are adjusted by a factor of one-half when using *f* = 0.5, which is a desirable option because it mirrors the 50% head start normally recommended for FIR. Setting the adjustment value, *α*, so that the FIR adjustment has very little impact after observation 20, such as F_{adj} at observation 20 will be 0.99, would be a fair setting. This ought to be adequate to enable the identification of quality issues at startup. According to this concept, we ought to fix $\alpha = \frac{(-\frac{2}{\log(1-f)}-1)}{19}$ (3.21)

when *f* = 0.5, *α*=0.3 is produced.

The ARL values for out-of-control processes have greatly improved with the introduction of the FIR feature in EWMA control charts, since FIR chooses a starting value that is not zero. The procedure's value would be its capacity to more promptly recognize a process that isn't on target when it starts, albeit at the expense of an increased rate of false alarms.

In order to improve also the false alarms simultaneously, two out of two runs rule technique is also used:

A run is typically defined as a collection of observations of the same type. We may specify the types of observations in addition to runs up and down as those above and below the center line, so that two points consecutively above the center line would constitute a run of length 2.

2/2 runs rules is the situation where a signal is given when any two charting statistics either: (i) both fall on or above (below) the UCL (LCL), or (ii) one falls on or above (below) the UCL (LCL) and the next one falls on or below (above) the LCL (UCL). (Adeoti, O. A., & Malela-Majika, J.-C. (2019))

The proposed scheme's design structure is as follows: a process is said to be out-of-control whenever two successive points plot either below the LCL_{fir} or above the UCL_{fir} .

The control limits are constructed as:

$$UCL_{fir} = \mu_0 + F_{adj}\sqrt{\frac{\lambda\mu_0}{2-\lambda}[1-(1-\lambda)^{2i}]} \qquad (3.22)$$

$$LCL_{fir} = \mu_0 - F_{adj}\sqrt{\frac{\lambda\mu_0}{2-\lambda}[1-(1-\lambda)^{2i}]}$$

where F_{adj} stands for FIR feature

Some of the findings from the comparison of the three EWMAs in terms of ARL_1 are shown in Table 3.6. With different combinations of μ and λ, the responses of the control charts to shifts in the process mean are discernible. The actual procedure mean μ_0 is 4. We should also point out that the time-varying control limits were employed to compare all three of these EWMAs, which are described previously in subsections 3.2 and 3.3.

It is advised to set a common in-control ARL for the charts in order to compare the performance of two or more control charts effectively. Here, ARL_0 was set to 200.

Table 3.6: Comparison of ARL_1 values of Poisson EWMA charts using different combinations of μ and λ when μ_0 is 4

μ	λ	Classical PEWMA	Double PEWMA	RR FIR PEWMA
4.5	0.05	44.99	$\boxed{41.34}$	43.28
	0.3	$\boxed{58.52}$	$\boxed{58.59}$	61.71
	0.5	65.36	$\boxed{62.23}$	70.10
5	0.05	16.23	15.20	$\boxed{14.43}$
	0.3	23.68	$\boxed{21.37}$	22.03
	0.5	28.67	$\boxed{24.71}$	26.97
6	0.05	5.78	5.23	$\boxed{4.26}$
	0.3	7.66	6.91	$\boxed{5.23}$
	0.5	9.08	7.87	$\boxed{6.21}$

According to Table 3.6, comparison reveals that the double PEWMA has lower out-of-control ARL values than the suggested chart in a very tiny region when the process shift has been lower or equal than 1 and the classical PEWMA has a superiority over the suggested scheme if the shift is lower or equal than 0.5. When there is more than one shift, RR FIR PEWMA is preferable to the other two.

One can observe that the control charts get more effective at spotting shifts as the weighting value drops.

Since most applications make it challenging to predict the values of process shifts, it is crucial that a control chart performs well across the whole process shift range rather than simply for a particular mean shift.

We will now present three more measurements for comparison of the control charts, which measure the overall performance:

- Average Extra Quadratic Loss (AEQL)

$$AEQL = \frac{1}{\delta_{max} - \delta_{min}} \int_{\delta_{min}}^{\delta_{max}} \delta^2 \, ARL(\delta) d\delta \qquad (3.23)$$

- Average Ratio of ARL (ARARL)

$$ARARL = \frac{1}{\delta_{max} - \delta_{min}} \int_{\delta_{min}}^{\delta_{max}} \frac{ARL(\delta)}{ARL_{best}(\delta)} d\delta \qquad (3.24)$$

- Performance Comparison Index (PCI)

$$PCI = \frac{AEQL}{AEQL_{best}} \qquad (3.25)$$

where δ is the difference between μ_1 (mean when the process is out-of control) and μ_0(mean when the process is in-control) and the best chart generates $ARL_{best}(\delta)$ and $AEQL_{best}$.

Table 3.7 shows the results, on the case where the process mean is μ_0=4 and smoothing constant λ = 0.05, 0.1, 0.2, 0.3, 0.4, and 0.5 with various L combinations, of the comparison of the proposed scheme denoted as RR FIR PEWMA (which stands for Run Rules with Fast Initial Response Poisson EWMA), the traditional PEWMA and DPEWMA in terms of the aforementioned measurements.

Table 3.7: Comparison of classical PEWMA, DPEWMA and RR FIR PEWMA when $\mu_0 = 4$

λ	Measurements	Classical PEWMA	Double PEWMA	RR FIR PEWMA

0.05	AEQL	24.222	21.977	$\boxed{16.128}$
	PCI	1.502	1.363	1.000
	ARARL	1.480	1.344	1.000
0.1	AEQL	26.155	24.039	$\boxed{17.246}$
	PCI	1.517	1.394	1.000
	ARARL	1.498	1.378	1.000
0.2	AEQL	29.716	27.524	$\boxed{18.629}$
	PCI	1.595	1.477	1.000
	ARARL	1.587	1.471	1.000
0.3	AEQL	31.428	28.624	$\boxed{20.006}$
	PCI	1.571	1.431	1.000
	ARARL	1.579	1.440	1.000
0.4	AEQL	33.586	30.846	$\boxed{30.846}$
	PCI	1.552	1.425	1.000
	ARARL	1.574	1.449	1.000
0.5	AEQL	36.065	31.899	$\boxed{23.636}$
	PCI	1.526	1.350	1.000
	ARARL	1.548	1.375	1.000

From Table 3.7 we can conclude that from a broad perspective, the proposed chart performs approximately twice as well as the PEWMA chart in terms of the AEQL, PCI, and ARARL. For instance, when $\lambda = 0.1$, the proposed chart outperforms the traditional PEWMA in terms of PCI by 51.7%.The total performance, as measured by the AEQL, PCI, and ARARL, actually shows that the double PEWMA chart is at least 34.4% less effective than the proposed graphic. For example, when $\lambda= 0.2$, the suggested method outperforms the double PEWMA by more than 47% in terms of PCI and ARARL.

https://doi.org/10.26219/heal.aueb.6224

In conclusion, double PEWMA is superior to the other two if the process mean only changes by a tiny amount, such as by 1. Overall chart performance shows that the RR FIR PEWMA performs better in terms of AEQL, ARARL, and PCI.

3.5 Control Charts with Ranked Set Sampling Technique

All of the aforementioned control charts are predicated on the notion that the data collection method employed was Simple Random Sampling (SRS).

According to Montgomery (2009), in Simple Random Sampling the units from the lot that are chosen at random for inspection must be representative of all the goods in the lot. This is how bias will be reduced. To be more specific, SRS is made to make sure that every person in a group has the same and separate opportunity to be chosen for a small group to study and this is making it a fair and unbiased way of selecting . By using this method, researchers are able to select samples that accurately represent the population's traits. This helps them make trustworthy conclusions and general statements.

But literature has demonstrated that Ranked Set Sampling (RSS) is more efficient.

Ranked set sampling (RSS) is a way to choose a sample from a group of things. It combines random selection with putting the things in order. This method tries to make the estimation process more accurate and efficient by using the rankings. When using this technique, the group of things is split into smaller groups called "ranks" or "sets. " In each rank, a random sample is taken, and the things within that rank are put in order. We do the rank sampling process multiple times to get many sets of ranked observations. The size of each rank can be different, but it is usually not big.

The main concept of RSS is that instead of looking at individual measurements, we can compare rankings to better understand the relative sizes of the observations. Instead of gathering many separate measurements, RSS lets researchers choose and organize smaller groups of data, which saves time and effort.

After getting the ranked sets, we can do statistical analysis by using the ranks instead of the original measurements. RSS gives us unbiased estimations for population numbers and often gives us more accurate estimations compared to SRS. It can be very helpful in situations where the relationship between observations in order provides important information about the group we are interested in.

 https://doi.org/10.26219/heal.aueb.6224

3.5.1 PEWMA control chart based on RSS technique

Abujiya et al.(2016) suggested a new PEWMA chart for tracking the process mean using RSS approach in order to increase the sensitivity of the conventional PEWMA chart to various types of changes in Poisson processes, named as RPEWMA.

The traditional PEWMA control chart, that is described in subchapter 3.2, is based on simple random samples, and its design procedure can be applied to single observations or rational subgroups.

Let $X_{(j:n)i}$ represent the *jth* order statistic for the *jth* sample of subgroup size n in the *ith* cycle from the Poisson distribution with parameter μ where *j=1,..,n* and *i=1,…,m*.

Then, an unbiased estimator for the mean μ of *jth* cycle is:

$$\widehat{\mu_{SRSi}}=\frac{\sum_{j=1}^{n} x_{\mathrm{ji}}}{n} \text{ with } Var(\widehat{\mu_{SRSi}}) = \frac{\mu}{n} \tag{3.26}$$

We must also emphasize that now we do have μ_{SRS} instead of μ in order to distinguish the two techniques which are used. As before, if the process is in-control $\mu=\mu_0$ and out of-control if $\mu=\mu_1$.In case where n=1, we get $\widehat{\mu_{SRSi}} = X_i$ as we previously had in equation (3.1).

The traditional PEWMA chart for tracking the process mean, based on the statistic is:

$$Z_{SRS_i} = \lambda \cdot \widehat{\mu_{SRSi}} + (1-\lambda) \cdot Z_{SRS_{i-1}} \quad for\ i = 1..m \tag{3.27}$$

$$Z_{SRS_0} = \mu_0$$

where the smoothing constant λ takes values in (0,1] and specifies the amount of memory that the EWMA structure contains.

Therefore, due to the fact that the observations are independent, the variance of Z_{SRS_i} is:

$$Var(Z_{SRS_i}) = \frac{\lambda}{2-\lambda}\left[1-(1-\lambda)^{2i}\right]\frac{\mu_0}{n} \tag{3.28}$$

Consequently, the time-varying control limits are:

$$UCL_{SRS} = \mu_0 + L\sqrt{Var(Z_{SRS_i})} \tag{3.29}$$

$$Center\ Line = \mu_0$$

$$LCL_{SRS} = \mu_0 - L\sqrt{Var(Z_{SRS_i})}$$

 https://doi.org/10.26219/heal.aueb.6224

For the construction of the RPEWMA, instead of using the estimator in equation (3.25) we will use the unbiased linear estimate for the Poisson process mean, utilizing RSS data, which is expressed as:

$$\widehat{\mu_{RSS\,i}} = \frac{\gamma_n}{n} \sum_{j=1}^{n} X_{(j:\,n)i} \tag{3.30}$$

where γ_n=(1/n)$\sum_{j=1}^{n} \gamma_{(j:n)}$ is a correction factor that has been chosen to minimize Var($\widehat{\mu_{RSS\,i}}$), the variance of the *jth* sample of a subgroup with size *n*. In this research, γ_n is discovered to be roughly equal to one.

Now, the variance of $\widehat{\mu_{RSS}}$ is :

$$Var(\widehat{\mu_{RSS}}) = \frac{\lambda \sum_{j=1}^{n} \frac{{a_{(j:n)}}^2}{b_{(j:n)}}}{\left(\sum_{j=1}^{n} \frac{1}{b_{(j:n)}}\right)\left(\sum_{j=1}^{n} \frac{{a_{(j:n)}}^2}{b_{(j:n)}}\right) - \left(\sum_{j=1}^{n} \frac{a_{(j:n)}}{b_{(j:n)}}\right)^2} \tag{3.31}$$

where $a_{(j:n)}$ *and* $b_{(j:n)}$ stand for the mean and variance of the reduced ordered variable $\eta_{(j:\,n)i} = \frac{X_{(j:\,n)i} - \mu}{\sqrt{\mu}}$.

Assume that the preliminary in-control Poisson process data can be used to estimate the process mean 0 or that it is known.

Also, consider the possibility that the process variance is well-known and consistent. We define the novel RPEWMA control statistic based on RSS for tracking changes in the Poisson process mean as follows in a setup analogous to the classical one:

$$Z_{RSS\,i} = \lambda \cdot \widehat{\mu_{RSS\,i}} + (1-\lambda) \cdot Z_{RRS\,i-1} \; for \; i = 1,..,m \tag{3.32}$$

$$Z_{RSS0} = \mu_0$$

The new control limits of RPEWMA are the following:

$$UCL_{RSS} = \mu_0 + L\sqrt{Var(Z_{RSS\,i})} \tag{3.33}$$

$$LCL_{RSS} = \mu_0 - L\sqrt{Var(Z_{RSS\,i})}$$

with $Var(Z_{RSS\,i}) = \frac{\lambda}{2-\lambda}\left[1-(1-\lambda)^{2i}\right] Var(\widehat{\mu_{RSS\,i}})$ (3.34)

Table 3.8 contains some comparison results between the proposed RPEWMA, the traditional PEWMA, and the PDEWMA, in terms of ARL_1. The real process mean is $\mu_0 = 8$, ARL_0 is set to be about equal to 200 in all three cases, *n*=5 and the weighting parameter λ is 0.05 and 0.5.

https://doi.org/10.26219/heal.aueb.6224

Table 3.8: Comparison of RPEWMA, PEWMA and PDEWMA when the process mean is $\mu_0 = 8$

μ	λ	RPEWMA	Classical PEWMA	Double PEWMA
6	0.05	4.41	10.20	8.10
	0.50	2.98	57.40	22.30
8	0.05	201.48	200.20	200.20
	0.50	199.46	200.60	200.10
9	0.05	9.45	27.90	24.50
	0.50	10.46	50.40	44.90
11	0.05	3.05	3.50	2.90
	0.50	1.76	4.90	4.40

From the comparison between PEWMA, PDEWMA and RPEWMA, which are introduced in Table 3.8, in terms of RL, results indicate that the suggested RPEWMA chart is more effective at identifying both the positive and negative changes in a Poisson process. More specifically, we notice that the inertia problem, which has worst cases for greater values of λ, makes the classical PEWMA more effective at identifying upward shifts than downward shifts. Additionally, when it comes to identifying rises and decreases in the mean of a Poisson process, PDEWMA is more efficient than the traditional PEWMA chart. Comparing also reveals that the suggested RPEWMA chart dominates the PDEWMA chart since they both have smaller ARL_1 values, with the exception for big shifts when a very tiny smoothing constant λ=0.05 is applied. As a conclusion, the new PEWMA using RSS technique outperforms the older schemes.

3.5.2 Combination of Shewhart's and PEWMA using RSS Technique

Unquestionably, the Shewhart's control charts continue to be the method for quality control that is most frequently employed. Up to this point, whenever we mentioned Shewhart's control in this chapter, we were referring to the c-chart because the sample size was 1. The Shewhart's u-chart is the most straightforward control chart for tracking a Poisson process' rational subgroup.

https://doi.org/10.26219/heal.aueb.6224

The u-chart, like other Shewhart's control charts, is only sensitive to significant changes in the process since it only uses data from the most recent sampled product, ignoring all previous data. Many scholars have looked at different options that take information from both the past and present samples, such as the Poisson exponentially weighted moving average (PEWMA) control charts, for minor to moderate shifts in a Poisson process.

Many authors have advocated using the Shewhart's and EWMA control charts together to guide against all types of shifts in a process. Abujiya (2017) tried to combine RSS technique with Shewhart's u-chart and PEWMA, denoted as RSS CS-PEWMA.

Once again he used the unbiased linear estimate for the Poisson process mean as described in (3.29) which is $\widehat{\mu_{RSS\,i}} = \overline{X_{RSS_i}} = \frac{\gamma_n}{n}\sum_{j=1}^{n} X_{(j:n)i}$ and the variance which is described in (3.30) which is:

$$Var(\widehat{\mu_{RSS}}) = Var(\overline{X_{RSS_i}}) = \frac{\lambda \sum_{j=1}^{n} \frac{a_{(j:n)}^{2}}{b_{(j:n)}}}{\left(\sum_{j=1}^{n}\frac{1}{b_{(j:n)}}\right)\left(\sum_{j=1}^{n}\frac{a_{(j:n)}^{2}}{b_{(j:n)}}\right) - \left(\sum_{j=1}^{n}\frac{a_{(j:n)}}{b_{(j:n)}}\right)^{2}} \tag{3.35}$$

where $a_{(j:n)}$ and $b_{(j:n)}$ stand for the mean and variance of the reduced ordered variable $\eta_{(j:n)i} = \frac{X_{(j:n)i} - \mu}{\sqrt{\mu}}$, as before.

However the difference now, compared with the proposed scheme in 3.5.1, is when $\bar{X}_{RSSj}$ deviates from the ranges between the Shewhart u-chart control boundaries, the RSS CS-PEWMA chart alerts:

$$UCL_{RSS-S} = \mu_0 + K\sqrt{Var(\bar{X}_{RSS\,i})} \tag{3.36}$$

$$LCL_{RSS-S} = \mu_0 - K\sqrt{Var(\bar{X}_{RSS\,i})}$$

Or whenever the RSS PEWMA statistic which is

$$Z_{RSS\,i} = \lambda \cdot \bar{X}_{RSSj} + (1-\lambda) \cdot Z_{RRS\,i-1} \tag{3.37}$$

plots outside of the ranges between the control limits:

$$UCL_{RSS-E} = \mu_0 + L\sqrt{\frac{\lambda}{2-\lambda}[1-(1-\lambda)^{2i}]Var(\bar{X}_{RSS\,i})} \tag{3.38}$$

$$LCL_{RSS-E} = \mu_0 - L\sqrt{\frac{\lambda}{2-\lambda}[1-(1-\lambda)^{2i}]Var(\bar{X}_{RSS\,i})}$$

The study used run length properties such as Average Run Length (ARL), Standard Deviation of Run Length (SDRL) and Median Run Length (MDRL) and also metrics

https://doi.org/10.26219/heal.aueb.6224

for the overall performance such as AEQL, ARARL and PCI which were introduced in subchapter 3.4.The comparison between the classical PEWMA, the classical CS-PEWMA and the novel scheme RSS CS- PEWMA shows that not only the RSS CS-PEWMA has a superiority over the other two in terms of ARL_1, but the scheme also seems to be more symmetrical than the traditional charts, which becomes more obvious as λ value increases. Overall, the suggested RSS CS-PEWMA chart is more effective in detecting changes in the Poisson process mean, than the other two, when seen in terms of PCI.

3.6 Triple Poisson EWMA control chart

The triple EWMA (TEWMA) chart for normally distributed data was recently developed by Alevizakos et al.(2021) in an effort to improve the detection efficiency of the traditional EWMA chart. Using this as a trigger, Alevizakos et al.(2022) suggested using a triple exponentially weighted moving average control chart for Poisson observations, regarded as PTEWMA chart.

The PTEWMA control chart's charting statistic is defined by the system of equations:

$$Y_i = \lambda \cdot X_i + (1-\lambda) \cdot Y_{i-1} \tag{3.39}$$

$$Z_i = \lambda \cdot Y_i + (1-\lambda) \cdot Z_{i-1}$$

$$W_i = \lambda \cdot Z_i + (1-\lambda) \cdot W_{i-1}$$

$$Z_0 = Y_0 = W_0 = \mu_0 \quad \textit{for i=1,2,....}$$

The statistics can also be written as:

$$Y_i = \lambda \cdot \sum_{j=0}^{i-1} (1-\lambda)^j \cdot X_i + (1-\lambda)^i \cdot Y_{i-1} \tag{3.40}$$

$$Z_i = \lambda \cdot \sum_{j=0}^{i-1} (1-\lambda)^j \cdot Y_i + (1-\lambda)^i \cdot Z_{i-1}$$

$$W_i = \lambda \cdot \sum_{j=0}^{i-1} (1-\lambda)^j \cdot Z_i + (1-\lambda)^i \cdot W_{i-1}$$

The time varying control limits are:

$$UCL_i = \mu_0 + L\sqrt{Var(W_i|\mu = \mu_0)} \tag{3.41}$$

$$\textit{Center Line}=\mu_0$$

$$LCL_i = \mu_0 + L\sqrt{Var(W_i|\mu = \mu_0)}$$

If the process has been running for several times, then the asymptotic control limits are:

$$UCL = \mu_0 + L\sqrt{\mu_0\left[\frac{6(1-\lambda)^6\lambda}{(2-\lambda)^5} + \frac{12(1-\lambda)^4\lambda^2}{(2-\lambda)^4} + \frac{7(1-\lambda)^2\lambda^3}{(2-\lambda)^3} + \frac{\lambda^4}{(2-\lambda)^2}\right]} \quad (3.42)$$

$$LCL = \mu_0 - L\sqrt{\mu_0\left[\frac{6(1-\lambda)^6\lambda}{(2-\lambda)^5} + \frac{12(1-\lambda)^4\lambda^2}{(2-\lambda)^4} + \frac{7(1-\lambda)^2\lambda^3}{(2-\lambda)^3} + \frac{\lambda^4}{(2-\lambda)^2}\right]}$$

In order to compare PTEWMA,PDEWMA and PEWMA, both two sided and one-sided charts, and draw meaningful conclusions, the ARL_0 is set at 370, and the competing charts are made utilizing time-varying control limits.

The findings of the comparison study are the followings:

In the case of two-sided charts, the PTEWMA chart is superior to the other two charts in detecting small downward shifts while the PEWMA chart is very effective in detecting a very small upward shift. Additionally, in both schemes, when the value of λ rises, the proposed chart is more sensitive than its rivals in a wider range of shifts.

In the case of one-sided charts, while PDEWMA and PTEWMA outperform the PEWMA charts, the PTEWMA charts are more effective than the PDEWMA charts, especially for small shifts.

https://doi.org/10.26219/heal.aueb.6224

Chapter 4

EWMA control charts with time-varying sizes for Poisson processes

The detection of change for scenarios with count data when the area of sample size is not consistent over time or are closely connected to the amount of product exposure, is one area of interest in Quality Control. Let's consider the cases where one looks at the quantity of nonconformities in batches, but the batch size varies between samples or the frequency of negative drug reactions over a set period of time, where the higher the product exposure, the greater the likelihood of negative drug reactions. When creating these control charts, these scenarios must be taken into consideration. In this chapter, some EWMA control charts with time-varying sizes for Poisson observations will be introduced.

4.1 Shewhart's control chart adaption for time-varying sample sizes

Fistly, it must be punctuated that either the problem is in the sample sizes or the product exposure, all of the described control charts are applicable to each of these situations. Therefore, for convenience and reasons for understanding, we will say only for sample sizes.

Occasionally, control charts for nonconformities are created utilizing a 100% product inspection. The number of inspection units in a sample will often vary when this sampling technique is applied. If a control chart for nonconformities, such as c-chart, is used, the center line and the control limits will change depending on the sample size. This type of control chart would be quite challenging to interpret. Utilizing a control chart for nonconformities per unit is the proper technique, such as u-chart.

Let X_i be the collected statistic at time *i=1,…*

We assume that $X_{1,}X_2$.. are independent Poisson observations and $n_{1,}n_2$.. are the sample sizes respectively. We also suppose that each X_i follows a Poisson distribution with in-control process mean equals to $n_i * \mu_0$ and out-of control mean equals to $n_i * \mu_1$. Then, $\mu_1 > \mu_0$ since we are interested only in the increase of the number of nonconformities in an inspection unit.

Suppose we have a changepoint *r* that the mean changes from μ_0 to μ_1 .

Then,

$$X_i \sim \begin{cases} Poisson(n_i * \mu_0), & for\ i = 1,2 \ldots r \\ Poisson(n_i * \mu_1), & for\ i = r+1, \ldots \end{cases} \tag{4.1}$$

 https://doi.org/10.26219/heal.aueb.6224

The time-varying control limits for the Shewhart's u-chart is :

$$UCL_i = \mu_0 + L\sqrt{\frac{\mu_0}{n_i}} \tag{4.2}$$

$$LCL_i = \mu_0 - L\sqrt{\frac{\mu_0}{n_i}}$$

for i=m+1,m+2..

where L is usually equals to 3 due to the three sigma limits and m is the number of observations until a point exceeds the control limits in Phase I.

If LCL value is negative, we set it to zero, just like any other control chart we have discussed.

4.2 EWMA control charts for varying sample sizes

Even though, u-chart can be used to analyze procedures with different sample sizes in Phase I and Phase II control charting, generally Shewhart's charts are less sensitive to detecting tiny parameter shifts during Phase II studies, which is a major drawback since we need to detect the change as soon as feasible. Therefore, during Phase II investigations, more sensitive charts like exponentially weighted moving average (EWMA) control charts are frequently used.

In the case of various sample sizes, Dong et al.(2008) proposed the recursion for EWMA to be defined as :

$$Z_i = (1-\lambda)\cdot Z_{i-1} + \lambda \cdot \frac{X_i}{n_i} + \quad for\ i = 1,2.. \tag{4.3}$$

$$Z_0 = \mu_0$$

Or $$Z_i = (1-\lambda)^i \cdot \mu_0 + \lambda \sum_{j=1}^{i}(1-\lambda)^{i-j}\, \frac{X_j}{n_j} \tag{4.4}$$

where

Z_i is EWMA statistic at time *i*

μ_0 is starting value or target value (occasionally, the mean of historical data is used)

X_i is the collected statistic at time *i*

n_i is the sample size at time *i*

https://doi.org/10.26219/heal.aueb.6224

λ is a smoothing parameter which takes values in (0,1] and determines the depth of memory of EWMA

When the process is in-control, which means that the mean of Z_i is μ_0, the variance of Z_i is calculated as:

$$\sigma_{Z_i}^2 = Var(Z_i) = \lambda^2 \sum_{j=1}^{i} (1-\lambda)^{2i-2j} \frac{\mu_0}{n_j} \tag{4.5}$$

As i increases we do have:

$$\lim_{i\to\infty} \lambda^2 \sum_{j=1}^{i} (1-\lambda)^{2i-2j} \frac{\mu_0}{n_j} = \frac{\mu_0}{n_0} \frac{\lambda}{2-\lambda} \tag{4.6}$$

where n_0 is the minimum of all the sample sizes for i = 1,2..

We must exercise extreme caution while selecting λ. A small value of λ, close to 0, in an EWMA raises one possible issue. Because the small l does not give the new data much weight, it may take the EWMA several periods to respond to a shift in the mean that occurs when the value of the EWMA is on one side of the center line. This is called the inertia effect. It may impair the EWMA's capacity for shift detection. However, if λ is set to a large value, close to 1, it may take longer to detect a small shift. According to Montgomery (2009), the best choice for λ would be in the interval [0.05,0.25].

4.3 Uniformly distributed sample sizes

Dong et al. (2008) investigated three distinct control limit strategies. They only employed UCLs for the three techniques because they were specifically interested in identifying an increase in the incidence rate.

The first strategy is called EWMAe-type and has the following UCL:

$$UCL_{1,i} = \mu_0 + L_1 \sqrt{\lambda^2 \sum_{j=1}^{i} (1-\lambda)^{2i-2j} \frac{\mu_0}{n_j}} \tag{4.7}$$

The second approach is known as EWMAa1-type and has the subsequent UCL:

$$UCL_{2,i} = \mu_0 + L_2 \sqrt{\frac{\mu_0}{n_0} \frac{\lambda}{2-\lambda} [1-(1-\lambda)^{2i}]} \tag{4.8}$$

The third technique, which uses the asymptotic variance of Z_i when i increases to infinity from equation (4.6), has been named as EWMAa2-type and includes the following UCL:

https://doi.org/10.26219/heal.aueb.6224

$$UCL_{3=}\mu_0 \; + L_3\sqrt{\frac{\mu_0}{n_0}\frac{\lambda}{2-\lambda}} \tag{4.9}$$

We must keep in mind that all the three approaches are equal when the sample size is constant, and when λ=1 EWMAa1-type and EWMAa2-type are same.

However there are two significant problems in the use of this control limits. The first one is that the ultimate goal of the EWMA control chart is hampered by the use of the minimal sample size in the control-limit calculations. However, EWMA has been developed in Phase II. This chart is useful for keeping track of a process that has been under control. Because the samples are being obtained in real-time, it follows that one will not be able to determine in advance the minimum sample size for the full set of .samples. To use these control limits described in (4.8) and (4.9), one must be aware of the minimum sample size. The second issue is that because they are only concerned with identifying an increased rate, they just erase the LCL. The absence of this limit allows the EWMA statistics to take on very small values, which could lead to serious inertial problems, particularly if λ is small.

Ryan and Woodall (2010) suggested utilizing a novel EWMA approach that is distinct from the EWMA approaches aforementioned in equations (4.8) and (4.9). Their modified EWMA method, which they refer to as the modified EWMA method, EWMA-M, are dependent on the precise variance of the EWMA statistic, as shown in Equation (4.7) and the use of a lower reflecting barrier at $Z_i = \mu_0$.

A comparison between the EWMA-M, with different values of λ, and EWMAe-type with the proposed value of λ=0.9 by Dong et al.(2008) was made. The measure of evaluation that was used was ARL, and specifically steady-state ARL values, that are based on delayed shifts in the parameter instead of zero-state ARL values which are due to sustained shifts in the parameter that happen under the control chart's initial startup conditions.

At first, fixed sample sizes were employed to compare the new EWMA-M and EWMAa2-type. Keep in mind that the three EWMA control charts suggested by Dong et al.(2008) coincide when the sample sizes are constant.

It is clear that the EWMA-M chart's effectiveness for tracking Poisson counts with constant sample sizes is significantly impacted by the lower smoothing constant and the lower reflecting barrier. Additionally noted were several elevated EWMAa2-type ARL values. It may also be due to the absence of a reflecting lower barrier. The proposed schemes of Gan (1990) and Borror et al. were also compared (1998). It is discovered that the ARL values for EWMA-M were typically 10% higher than those for approaches that have both upper and lower bounds for a given increase in the parameter.

https://doi.org/10.26219/heal.aueb.6224

For the case of non constant sample sizes, we must also note that, in order to account for the different sample sizes n_i, a continuous uniform distribution *U(a,b)* was used in the interval of *(a,b)=(10,15)*. We looked at random sample sizes as opposed to monotonically growing or decreasing sample sizes. The lower bound a of 10 was chosen because Dong et al.(2008) study employed the same minimum sample size. The zero state ARL_0 was set to 200.

Table 4.1 represents some of the results where μ_0 is 1 and μ_1 is 1.2, 1.5, 1.8 and 2.

Table 4.1: Comparison of ARL values between EWMA-M and EWMAe for $\mu_0 = 1$ and $\mu_1 = 1.2, 1.5, 1.8$ and 2

μ_1	EWMA-M λ=0.05	EWMA-M λ=0.1	EWMA-M λ=0.15	EWMA-M λ=0.2	EWMA-M λ=0.5	EWMAe λ=0.90
1.2	$\boxed{11.53}$	$\boxed{11.48}$	11.80	$\boxed{12.56}$	18.38	26.79
1.5	4.12	3.68	3.46	$\boxed{3.44}$	-	4.66
1.8	2.62	2.32	2.15	2.03	$\boxed{1.85}$	1.98
2	2.15	1.90	1.74	1.66	$\boxed{1.44}$	$\boxed{1.45}$

Due to the fact that sample sizes n_i are varying , by extension shifts in the Poisson mean, $n_i * \mu_1$, will vary. The findings in Table 4.1 indicate that the EWMA-M method is more sensitive to tiny shifts when the smoothing constants are smaller. The EWMA-M chart with λ =0.5 has the shortest detection time among the various EWMA techniques as μ_1 increases. The need to select the smoothing constant based on the magnitude of the shift one desires to detect is once again made clear by this. Both the EWMA-M chart and the EWMAe chart function similarly at the shift where $\mu_1 = 2$. Additionally, they compared the new EWMA-M with EWMAa2 type control chart. To determine whether altering the uniform distribution's characteristics had any effect on the relative ARL performance of the control-chart approaches in this study, both the *U(10, 20)* and *U(10, 50)* examples were investigated. The EWMAa2 approach performed much better than the other control chart methods when the value of *b* was increased to 20 and 50 and the shift of interest was significant. Because the shift in the means of the Poisson random variables rises as sample sizes grow, the EWMAa2 technique performs better.

As a conclusion, the newly developed EWMA-M charts provide good ARL characteristics for identifying different parameter shifts for both fixed and non fixed sample sizes. The EWMA-M chart has several features, including control limits based on the precise variance of the EWMA statistics, a reflecting lower barrier to secure against inertial issues, and a smoothing constant for the chart related to the main shift of interest. These features eliminate the problem of an unknown minimum sample size in Phase II.

https://doi.org/10.26219/heal.aueb.6224

4.4 In view of the variability of the sample sizes

Despite the fact that the EWMAe and EWMA-M charts are extremely sensitive to parameter modification, one can ask how to properly create an EWMA scheme by taking into account the variability of the sample sizes. Keep in mind that the observed numbers in these two charts are divided by the respective sample sizes. It makes sense since the goal of this process is to create a series of random variables with constant expectation over time, similar to the conventional EWMA charts for normal observations.

In order to account for the variability of the sample sizes, the main idea of Dong et al. (2008) and Ryan and Woodall (2010) was to split the observed counts by the corresponding sample sizes. A new EWMA control chart was proposed by Zhou et al. (2012) that naturally combines time-varying sample sizes with the EWMA scheme that may be developed under the weighted likelihood framework which its very nature takes into account different sample sizes when developing the scheme for tracking Poisson count data. This EWMA chart has an advantage in identifying recent parameter changes because the weighted likelihood method ignores prior data concerning change points.

Once again, we assume that $X_{1,}X_2$.. are independent Poisson observations and $n_{1,}n_2$.. are the sample sizes respectively. We also suppose that each X_i follows a Poisson distribution with in-control process mean equals to $n_i * \mu_0$ and out-of control mean equals to $n_i * \mu_1$ where μ_0 is the frequency of a rare occurrence and μ_1 an unknown value that μ_0 changes to in an unknown time *r* with $\mu_1 > \mu_0$.

Yet again from equation (4.1):

$$X_i \sim \begin{cases} Poisson(n_i * \mu_0), & for\ i = 1,2 \ldots r \\ Poisson(n_i * \mu_1), & for\ i = r+1, \ldots \end{cases}$$

In terms of hypothesis testing we do have:

$$H_0 : \mu = \mu_0 \tag{4.10}$$

$$H_1 : \mu \neq \mu_0$$

at each time point.

Then, the log likelihood of each observation X_j , by ignoring two constant terms with respect to θ, is:

$$l_j(\mu) = X_j \log \mu - n_j \mu \tag{4.11}$$

Therefore, the weighted log-likelihood over samples 1 to *i*, at any time point *i* is:

 https://doi.org/10.26219/heal.aueb.6224

$$Y_i(\mu;\lambda) = \sum_{j=0}^{i} \omega_{j,\lambda} l_j(\mu) \tag{4.12}$$

where :

λ is the smoothing parameter and takes values between (0,1]

$\omega_{j,\lambda} = \lambda(1-\lambda)^{i-j}$ is a series of constants which is used to guarantee that the weights add up to 1 as i increases to infinity.

The following maximization issue is defined as the maximum weighted likelihood estimate, MWLE, of at the time point i given the value of λ:

$$\widehat{\mu_i} = argmax_\mu Y_i(\mu,\lambda) \tag{4.13}$$

Doing some calculations we get:

$$\widehat{\mu_i} = \frac{\sum_{j=0}^{i} \omega_{j,\lambda} X_j}{\sum_{j=0}^{i} \omega_{j,\lambda} n_j} = \frac{Y_{c,i}}{Y_{p,i}} \tag{4.14}$$

Where $Y_{p,i}$ and $Y_{c,i}$ are the population's and counts' exponentially weighted average, correspondingly.

As a result we get the weighted likelihood ratio test (WLRT), represented as $R_{i,\lambda}$ which is:

$$\begin{aligned} R_{i,\lambda} &= 2[Y_i(\widehat{\mu_i};\lambda) - Y_i(\mu_0\,;\lambda)] \\ &= 2\sum_{j=0}^{i} \omega_{j,\lambda}\left[l_j(\widehat{\mu_i}) - l_j(\mu_0\,)\right] \\ &= 2[Y_{c,i} \log\frac{Y_{c,i}}{\mu_0\, Y_{p,i}} - Y_{c,i} + \mu_0\, Y_{p,i} \end{aligned} \tag{4.15}$$

The WLRT value $R_{i,\lambda}$, can be utilized as the monitoring statistic, and the associated control chart sends a signal if $R_{i,\lambda}$ goes over a predetermined control limit. We will refer to this control chart as WRLT-based EWMA, denoted as WEWMA.

We should also mention that $Y_{p,i}$ and $Y_{c,i}$ can be expressed also as:

$$Y_{c,i} = \lambda X_j + (1-\lambda) Y_{c,i-1} \tag{4.16}$$

$$Y_{c,0} = \mu_0\, n_1$$

$$Y_{p,i} = \lambda n_j + (1-\lambda) Y_{p,i-1} \tag{4.17}$$

$$Y_{p,0} = n_1$$

 https://doi.org/10.26219/heal.aueb.6224

As a consequence, the WEWMA control chart can still be used in a recursive manner, much like standard EWMA charts.

As previously said, in practice, we are frequently just interested in identifying a rise in the occurrence rate, so a one-sided chart is preferable. Therefore, the hypothesis testing described in expression (4.10) takes the form of:

$$H_0 : \mu = \mu_0 \tag{4.18}$$

$$H_1 : \mu > \mu_0$$

Hence, Shu et al.(2012) modified the existing MWLE to:

$$\widetilde{\mu_i} = \widehat{\mu_i} I(\widehat{\mu_i} > \mu_0) + \mu_0 I(\widehat{\mu_i} \leq \mu_0) \tag{4.19}$$

because the function $Y_i(\mu\,; \lambda)$ decreases monotonically on the right side of μ_0 when $\widehat{\mu_i} \leq \mu_0$.

The WEWMA statistic now will be:

$$\tilde{R}_{i,\lambda} = R_{i,\lambda} I(\widehat{\mu_i} > \mu_0) \tag{4.20}$$

The novel one-sided proposed EWMA chart will alert if $\tilde{R}_{i,\lambda}$ exceeds the following upper control limit:

$$UCL_{WEWMA} = L\frac{\lambda}{\lambda - 2}\,, for\ i = 1{,}2.. \tag{4.21}$$

where L is selected to achieve a specific ARL_0.

For the comparison of the control charts, that were aforementioned in this chapter, various scenarios of time-varying sample sizes were used. Mei et al.(2011) recommended using the logistic model to model population growth. They were particularly interested in four models for the sample sizes: an increasing scenario, a fast increasing scenario, a decreasing and fixed.

4.4.1 In Control Performance

It is frequently insufficient to characterize run length behavior using ARL, particularly when the marginal distribution of the charting statistic is not the same for all time points t. For that reason more metrics of evaluation were used such as False alarm for the first 30 observations, Standard Deviation of Run Length (SDRL) and False Alarm Rate (FAR). According to Hawkins and Olwell (1998), the IC run length distribution is regarded satisfactory if it is near to the geometric distribution,

The findings suggest that:

https://doi.org/10.26219/heal.aueb.6224

- For the cases of 2 increasing scenarios, the SDRLs and FARs of EWMAa1 and EWMAa2 are significantly higher than the anticipated values. These figures are undesirable in terms of run length distributions since there are too many false alarms during early runs that will skew the detection results. The geometric distribution can also be observed to be a fairly good approximation to the IC run length distributions of the EWMAe, EWMA-M, and WEWMA charts.
- For the decreasing scenario, the geometric distribution is far from the run length distributions of EWMAa1 and EWMAa2. In this situation, their SDRLs are significantly smaller than the standard 300, which appears to be advantageous. Actually, this advantage stems from the fact that the chances of false alarms after short runs are extremely low, causing the chart to fail to detect shifts quickly.
- As we pointed out before when we have fixed sample sizes all the proposed charts from Dong et al.(2008) coincide. Therefore, the EWMAe, EWMA-M, and WEWMA charts provide adequate in-control run duration performance.

It is also observed that, the control limit coefficient L is affected not just by the control charts, but also by the underlying population models. When we define the control limit for a control chart, however, the actual population model is rarely known ahead of time. It is worth noting that, when compared to other alternative control charts, the WEWMA chart has a generally consistent control limit coefficient for various underlying population models.

4.4.2 Out of Control Performance

The EWMAa1 and EWMAa2 charts, as demonstrated in the previous section, have poor IC run length distributions. When compared to a geometric distribution, these EWMA adjustments accomplish the specified IC ARL with increased probabilities of very short and very long runs. When compared to the WEWMA and EWMAe charts, the OC model would reduce the likelihood of very long runs, resulting in relatively small ARLs. The ARL_0 was set to 300 with $\mu_0 = 1$.

The results show that:

- For the 2 increasing scenarios, for shifts up to $\mu_1 = 1.4$, the WEWMA chart performs better than all other control charts. When μ_1 is greater than 1.5, the EWMAM chart performs better than the WEWMA chart, and the WEWMA chart normally outperforms the EWMAe chart.
- Under the circumstances of decreasing and constant sample sizes, it is observed that the three EWMA charts have equivalent and comparable detecting abilities. The EWMA-M chart is more effective at identifying major

https://doi.org/10.26219/heal.aueb.6224

movements, whilst the EWMAe and WEWMA charts are more sensitive to small shifts.

Overall, WEWMA is not only more resilient in in-control, IC, and out of-control, OC, performance than existing techniques, but it is also more sensitive to tiny and moderate parameter changes. In many cases, the improvement is extremely significant. Generally, it outperforms the other competitors especially when sample sizes vary dramatically over time.

4.5 EWMA control chart with probability control limits

All of the work stated above was based on the presumption that the sample size adheres to a known random or deterministic model that is known a priori when setting appropriate control limits before to the start of the control charts. Traditional control charts are quite sensitive to the setting of sample sizes, as Zhou et al. (2012) noted. In reality, we often know very little about time-varying sample sizes. Estimating the sample size distribution function based on a collection of past data is a workable solution. The historical observations, however, are constrained, the estimation would invariably be faulty, and model misspecification or estimating mistakes would result in poor performance of the control charts.

Shen et al.(2013) recommended using probability control limits in an EWMA control chart for monitoring Poisson count data with time-varying sample sizes in Phase II process monitoring to overcome this difficulty. The suggested EWMA chart always shares an identical run length distribution with the geometric distribution, regardless of the unknown time-varying sample sizes and the fact that the false alarm rate is independent of monitoring time or sample size, and is thus known as the EWMAG chart since. Except for the intended false alarm rate, no sample size models must be specified before implementation. The basic idea behind their suggestion is to keep the conditional probability, the likelihood that the charting statistic will exceed the control limit if no alert occurs before the current time point, to the predefined false alarm rate at each time point.

Therefore now we have:

$$X_i \sim \begin{cases} Poisson(n_i * \mu_0 \mid n_i), & for\ i = 1,2 \dots r \\ Poisson(n_i * \mu_1 \mid n_i), & for\ i = r+1, \dots \end{cases} \tag{4.22}$$

The recursion they used is once again the one that Dong et al.(2008) proposed in equation (4.3) which is:

$$Z_i = (1-\lambda) \cdot Z_{i-1} + \lambda \cdot \frac{X_i}{n_i} + \quad for\ i = 1,2..$$

https://doi.org/10.26219/heal.aueb.6224

$$Z_0 = \mu_0$$

The EWMAG chart's control limit is configured to have a false alarm rate that is equal to the conditional probability, or the likelihood that the charting statistic will exceed the control limit in the absence of any prior alerts.

In mathematical terms we have the following equations:

$$\Pr(Z_1 > h_1(a)|n_1) = \Pr\big(Z_i > h_i(a)|Z_j > h_j(a), 1 \leq j \leq i, n_i\big) = a \;\;, for\ i > 1 \tag{4.23}$$

where :

a is the prespecified false alarm rate

$h(n_i)$ is a control limit based on previous data

Comparing the EWMAG chart's performance to that of the EWMAe and EWMAM charts under four scenarios of time-varying sample sizes, an increasing, a decreasing, a constant and a uniform.

4.5.1 In Control Performance

This is the same as conducting a type-I error hypothesis test for each time point *i*. As a result, the IC run length is the geometric distribution. The probability control limit at time *i* is established immediately after we observe the value of n_i. As a result, the EWMAG chart is not concerned with making incorrect assumptions or needing to predict future sample sizes.

Contrarily, under varied conditions, the curves of the other three control charts dramatically diverge from the geometric distribution curve to varying degrees. In all scenarios bar the decreasing one, the EWMAe chart frequently has higher probability of giving false alarms than the geometric distribution.

The inaccurate specification of the model population is something else that needs to be taken into consideration. Poor IC performance can also be caused by incorrectly selected distribution function parameters, even when proper models are used. As was previously said, it is uncommon in many applications to receive precise knowledge regarding future population sizes. As a result, run length distributions produced by control charts built on the premise that distribution functions of different population sizes are precisely known are inappropriate. This amply demonstrates the benefit of EWMAG chart.

4.5.2 Out of Control Performance

Only the EWMAe chart is compared in order to examine OC performance because it has a form that is identical to the EWMAG chart other than for the control limitations. Since it is unfair to compare different techniques in terms of OC ARL when their IC run length distributions differ greatly, assuming that the population sizes are precisely known in this situation. Regardless of the population scenarios, it is clear that the two control charts are equivalent in terms of OC performance. This shows that the suggested EWMAG chart may provide the needed IC run duration performance without degrading its capacity to detect changes. It is important to note at this point that the primary goal of the suggested dynamic technique is to achieve the theoretical geometric distribution for the IC run length distribution of a control chart rather than to enhance the chart's detection capabilities.

Due to the proposed EWMAG chart's targeted IC run length performance and competitive OC performance, it is advised using it.

4.6 Variable Sampling Interval Technique

In Chapter 2, several EWMA control charts for attributes have been described, but up until that point, no research on adaptive EWMA chart schemes had been published. Traditional control charts have evolved into adaptive control charts, which allow parts of the parameters to change over time. In the later ones, one or more chart parameters, like sample size, sampling interval and control limit factor, are made variable based on the most current information provided by the last point depicted.

Epprecht et al.(2009) proposed an adaptive control chart with variable sampling interval which is equivalent to the one-sided Poisson EWMA chart, suggested by Borror et al.(1998), with the deduction of LCL and the addition of a variable sampling interval technique. We will refer to this control chart as VSI c EWMA. The deduction of LCL is due to the fact that detecting tiny and moderate upward fluctuations in the process nonconformities rate as fast as feasible is the primary concern, and that one-sided charts will be more effective against such shifts than their two-sided control charts with the same ARL_0. Regarding downward movements, we believe that, while desired, their detection is not necessary and may be left to other approaches. For the one-sided Poisson EWMA chart we will refer to as FSI c EWMA, which stands for Fixed Sampling Interval.

As a reminder from subchapter 2.1, Borror et all’s upper control limit is:

$$UCL = \mu_0 + L\mu_0\sqrt{\frac{\lambda}{2-\lambda}} \tag{4.24}$$

As for the VSI c EWMA we will use the standard recursion of EWMA which is :

https://doi.org/10.26219/heal.aueb.6224

$$Z_i = \lambda \cdot X_i + (1 - \lambda) \cdot Z_{i-1} \; for \; i = 1,2.. \tag{4.25}$$

$$Z_0 = \mu_0$$

where:

Z_i is EWMA statistic at time *i*

μ_0 is starting value or target value (occasionally, the mean of historical data is used)

X_i is the number of nonconformities at time *i*

λ is a weighting parameter which takes values in (0,1] and determines the depth of memory of EWMA

The novel VSI c EWMA will have one control limit, the UCL, and one warning limit (WL) which are defined as:

$$UCL = \mu_0 + k\mu_0 \sqrt{\frac{\lambda}{2 - \lambda}} \tag{4.26}$$

$$WL = \mu_0 + w\mu_0 \sqrt{\frac{\lambda}{2 - \lambda}}$$

where:

k is a control limit factor

w is a warning limit factor and *w* < *k*

The control chart uses two sample intervals: a larger sampling interval h_L and a shorter sampling interval h_S. In order to determine which interval to be used each time, the location of the most recent EWMA value has a principal role.

If $Z_i \in (WL, UCL]$ then the subsequent sample is taken after h_S time. If $Z_i \leq WL$, the subsequent sample is taken after h_L time.

According to them, the basic concept is to wait longer to take the next sample when the process is less likely to be in control in order to compensate for the shorter sampling intervals and wait shorter when the process is more probably to be out of control in order to lessen the delay in detecting special causes.

The adjusted average time to signal, AATS, which is the expected amount of time to occur between the occurrence of an increase in the mean number of nonconformities and the signal indicated by the chart, is the performance metric adopted. This metric is used to compare charts and serves as the objective function that must be minimized in order to optimize the designs of the charts. The sampling frequency, which is also stated for the problem in this study using its inverse, *h*, is a further aspect of the issue.

https://doi.org/10.26219/heal.aueb.6224

H is the straightforward constant sample interval for the FSI chart. The average sample interval when the process is under control, $\bar{h}$, should be maintained at the predetermined value h in the context of the VSI chart.

The findings show that the VSI method can significantly reduce the AATS of the c EWMA chart for shifts between 1.5 and 4.0 in the range of values of μ_0 taken into account in this study. Additionally, the advantage of using the VSI technique will increase depending on how significantly the mean number of nonconformities increases. Finally, the AATS decreases are not inversely related to the h_S reductions. The marginal advantage diminishes along with h_S.Working with $h_S = 0.25 * \bar{h}$ is already incredibly successful. Due to the fact that excessively small sampling intervals may not be realistic in a number of real-world scenarios, this result is significant and convenient.

https://doi.org/10.26219/heal.aueb.6224

Chapter 5

EWMA control charts for Conway-Maxwell-Poisson Observations

The Poisson distribution is the most widely employed probability distribution for the modeling of count data. When the distribution's mean and variance are considered to be equal, this distribution fits the data the best. However, there are times when this presumption is broken, and as a result, the outcomes are questionable. Conway and Maxwell (1962) suggested a more adaptable two-parameter distribution, in the context of queuing systems, known as a COM-Poisson distribution in order to address this flaw of the Poisson distribution. In this chapter, some EWMA control charts for COM-Poisson will be introduced.

5.1 The Conway-Maxwell-Poisson Distribution

Overdispersion is a common problem in Poisson models. The term "overdispersion" denotes the occurrence of more variability in a data collection than would be expected by a given statistical model. The Poisson distribution has only one parameter and does not permit adjusting the variance independently of the mean. On the other hand, underdispersion indicates that there is less variance in the data than projected. In such cases, one feasible strategy is to utilize the Binomial distribution (or Bernoulli) for underdispersion and the Negative Binomial (or Geometric) distribution for overdispersion.

As an alternative, Conway and Maxwell (1962) extended the Poisson distribution, also known as the Conway-Maxwell-Poisson (COM-Poisson or CMP) distribution, by adding a parameter to account for overdispersion and underdispersion. Shmueli et al.(2005) reintroduced this distribution, thirty years after its first formulation, and noticed its various advantages, such as it belongs to both the exponential and two-parameter power series of distributions families, and it enables for sufficient statistics and other features to be neatly determined.

Let X be a random variable which follows COM-Poisson distribution.

Then, the probability mass function is:

$$\mathrm{P}(X = x \mid \mu, \nu) = \frac{\mu^x}{(x!)^\nu z(\mu, \nu)}, \mu > 0 \text{ } and \text{ } \nu \geq 0 \quad for \text{ } x = 0,1,2 \ldots \qquad (5.1)$$

where:

μ is a scale parameter

https://doi.org/10.26219/heal.aueb.6224

v is a dispersion parameter

$z(\mu, \nu) = \sum_{s=0}^{\infty} \frac{\mu^s}{(s!)^\nu}$ is a normalizing constant

It should be also mentioned that three significant distributions are special cases of COM-Poisson distribution and are listed in Table 5.1.

Table 5.1: Distributions as special case of COM-Poisson

Condition	***z(μ,ν)***	**P($X \mid \mu, \nu$)**	**Distribution**
$\mu < 1, \nu = 0$	$\sum_{s=0}^{\infty} \mu^s = \frac{1}{1-\mu}$	$\mu^x(1-\mu)$	Geometric
$\nu = 1$	$\sum_{s=0}^{\infty} \frac{\mu^s}{s!} = e^\mu$	$\frac{e^{-\mu}\mu^x}{x!}$	Poisson
$\nu \to \infty$	$1+\mu$	$\frac{\mu}{1+\mu}$	Bernoulli

Note that for v, a value greater than 1 handles the issue with underdispersed data and lower than 1 implies overdispersion.

The approximations of mean and the variance of X are, respectively:

$$E(X) = \mu \frac{\partial \log(z(\mu, \nu))}{\partial \mu} \cong \mu^{\frac{1}{\nu}} - \frac{\nu - 1}{2\nu} \tag{5.2}$$

$$Var(X) = \frac{\partial E(X)}{\partial \log \mu} \cong \frac{\mu^{\frac{1}{\nu}}}{\nu} \tag{5.3}$$

Sellers (2011) employed the COM-Poisson distribution in Shewhart's attribute control charts and concuded that the COM-Poisson control chart is flexible and a generalization of the p-chart, c-chart, and u-chart. Her proposed chart accommodated both overdispersed and underdispersed data. She developed and displayed the k-sigma control limits for the case $k = 3$. However, these limits are inapplicable and deceptive for the case of the asymmetric COM-Poisson distribution.

Later, Saghir et al.(2012) extended the work of Sellers (2011) and created the COM-Poisson charts' probability control limits and analyzed the impact of k-sigma. The results inferred that for the COM-Poisson distribution, control limits based on k-sigma

https://doi.org/10.26219/heal.aueb.6224

will frequently cause false alarms, cannot provide any appropriate lower control limits, and are less efficient in declaring a point lying outside the control limits when the parameter shifts adown. If the method of creating the count data indicates some extra-variation, the probability control limits should be applied rather than the k-sigma limitations.

Consequently, an adaptable control chart that can be utilized for both under-dispersed and over-dispersed data was required.

5.2 A Generalized EWMA control chart

On that ground, Saghir and Lin (2013) proposed a flexible generalized EWMA control chart, denoted as the GEWMA chart, on the basis of the COM-Poisson distribution for tracking the average number of nonconformities.

Let X_i , $i=1,2..$ be a sequence of quality inspections obtained from an ongoing production process. Then, the observations $X_1, X_2...$ are independent and identically distributed COM-Poisson random variables. When the process is in control $\mu=\mu_0$ and $\nu = \nu_0$.

The usual EWMA statistic takes the form of :

$$Z_i = \lambda \cdot X_i + (1-\lambda) \cdot Z_{i-1} \; for \; i = 1,2.. \tag{5.4}$$

$$Z_0 = \mu_0 \frac{\partial \log(z(\mu_0 , \nu_0))}{\partial \mu_0}$$

or

$$Z_i = \lambda \cdot \sum_{j=0}^{i-1} (1-\lambda)^j \cdot X_{i-j} + (1-\lambda)^i \cdot Z_0 \tag{5.5}$$

where

Z_i is EWMA statistic at time *i*

X_i is the collected statistic at time *i*

λ is the weighting parameter which takes values in (0,1] and determines the depth of memory of EWMA

Z_0 is the process mean value when in-control

As a result, the mean and the variance of the statistic Z_i are :

 https://doi.org/10.26219/heal.aueb.6224

$$E(Z_i) = \mu_0 \frac{\partial \log(z(\mu_0, \nu_0))}{\partial \mu_0} \tag{5.6}$$

$$Var(Z_i) = \frac{\lambda}{2-\lambda}\left[1-(1-\lambda)^{2i}\right]\frac{\partial E(X_i)}{\partial \mu_0} \tag{5.7}$$

The suggested EWMA chart's control limits are presented as :

$$UCL_i = \mu_0 \frac{\partial \log(z(\mu_0, \nu_0))}{\partial \mu_0} + L_U \sqrt{\frac{\frac{\partial E(X)}{\partial \mu_0}\lambda\left[1-(1-\lambda)^{2i}\right]}{2-\lambda}} \tag{5.8}$$

$$LCL_i = \mu_0 \frac{\partial \log(z(\mu_0, \nu_0))}{\partial \mu_0} - L_L \sqrt{\frac{\frac{\partial E(X)}{\partial \mu_0}\lambda\left[1-(1-\lambda)^{2i}\right]}{2-\lambda}}$$

As i increases,these limits approach steady-state values. Therefore, the mean and the variance of the EWMA statistic Z are:

$$E(Z) = \mu_0^{\frac{1}{\nu}} - \frac{\nu-1}{2\nu} \tag{5.9}$$

$$Var(Z) = \frac{\lambda}{2-\lambda}\left[\frac{\mu_0^{\frac{1}{\nu}}}{\nu}\right] \tag{5.10}$$

Then, the steady state control limits are :

$$UCL = \mu_0^{\frac{1}{\nu}} - \frac{\nu-1}{2\nu} + L_U \sqrt{\frac{\lambda\left[\frac{\mu_0^{\frac{1}{\nu}}}{\nu}\right]}{2-\lambda}} \tag{5.11}$$

$$LCL = \mu_0^{\frac{1}{\nu}} - \frac{\nu-1}{2\nu} - L_L \sqrt{\frac{\lambda\left[\frac{\mu_0^{\frac{1}{\nu}}}{\nu}\right]}{2-\lambda}}$$

It is common practice to set L_U and L_L to have equal values ($L_L = L_U = L$). If the computed value is less than zero, LCL is set to zero.

According on ARL values, it is observed that this flexible and GEWMA attribute control chart based on the COM-Poisson distribution is superior to the one proposed by Sellers(2011) for nearly all shifts. It is also worth noting that the PEWMA chart proposed by Borror et al.(1998), that presented in Chapter 2, is a special case of this chart when $v = 1$.

5.3 New techniques for improving the GEWMA

In order to enhance the efficiency of the GEWMA control chart, a variety of methods have been implemented.

5.3.1 Multiple Dependent Sampling

Multiple Dependent Sampling, denoted as MDS, is a well-established sampling scheme that is widely utilized within the field of statistical process control. The concept of MDS scheme, which is predicated on a conditional sampling procedure, was firstly introduced by Wortham and Baker (1976). Notably, this sampling approach diverges from existing sampling schemes in that its determination of the lot is not based on a definitive criterion: the state of disposition is contingent upon, not only the contemporary sample, but also on the outcomes of prior samples or forthcoming samples. This sampling scheme is deemed highly efficient in the sense of sample size.

The control chart under consideration is founded on the COM-Poisson distribution, operating within the MDS scheme while utilizing the EWMA statistic to measure the quantity of non-conformities arising from the manufacturing process.

Aslam et al. (2014) suggested an MDS $\bar{X}$-bar charts using double control limits. Given this, Aslam et al.(2016) combined the MDS sampling procedure with the EWMA technique.

The procedural methodology for this proposed chart is explicated in the following steps:

1. At time *i*, a randomly selected sample of size 1 is acquired and the frequency of non-conformities is quantified as X_i . The EWMA statistic is then calculated from equation (5.4).
2. It is stated that the process is out-of-control when $Z_i \geq UCL_1 \; or \; Z_i \leq LCL_1$ and in-control if $LCL_2 \leq Z_i \leq UCL_2$. If not, moving on to next step.
3. The process can be classified as under control if a consecutive series of subgro ups *i* are deemed to be under control. Declare the process to be out of control if not.

The procedure, that has been described above, utilizes two sets of control limits, one set of external and one of internal.

The external control limits can are contacted as:

$$UCL_1 = \left(\mu_0{}^{\frac{1}{\nu}} - \frac{\nu-1}{2\nu}\right) + k_1\sqrt{\frac{\lambda}{2-\lambda}\left[\frac{\mu_0{}^{\frac{1}{\nu}}}{\nu}\right]} \tag{5.12}$$

$$LCL_1 = \left(\mu_0{}^{\frac{1}{\nu}} - \frac{\nu-1}{2\nu}\right) - k_1\sqrt{\frac{\lambda}{2-\lambda}\left[\frac{\mu_0{}^{\frac{1}{\nu}}}{\nu}\right]}$$

and the internal limits are:

$$UCL_2 = \left(\mu_0{}^{\frac{1}{\nu}} - \frac{\nu-1}{2\nu}\right) + k_2\sqrt{\frac{\lambda}{2-\lambda}\left[\frac{\mu_0{}^{\frac{1}{\nu}}}{\nu}\right]} \tag{5.13}$$

$$LCL_2 = \left(\mu_0{}^{\frac{1}{\nu}} - \frac{\nu-1}{2\nu}\right) - k_2\sqrt{\frac{\lambda}{2-\lambda}\left[\frac{\mu_0{}^{\frac{1}{\nu}}}{\nu}\right]}$$

where k_1 and k_2 are the control constants. In the case where $k_1 = k_2$ and $i = 0$, the chart is an expansion of the chart suggested by Saghir and Lin(2013).

The probability of being declared in-control for the proposed chart is expressed as follows:

$$\begin{aligned} P_{in}{}^{0} = P(\,LCL_2 \le Z_i \le UCL_2) \\ + \{P(\,LCL_1 < Z_i < LCL_2) \\ + P(\,UCL_2 < Z_i < UCL_1)\}\{P(\,LCL_2 \le Z_i \le UCL_2)\}^i \end{aligned} \tag{5.14}$$

Therefore, the Average Run Length of the in-control process (ARL_0) may be computed as follows:

$$ARL_0 = \frac{1}{1 - P_{in}{}^{0}} \tag{5.15}$$

The probability of being stated out-of-control for the suggested chart is the following:

$$\begin{aligned} P_{in}{}^{1} = P(\,LCL_2 \le Z_i \le UCL_2)^c \\ + \{P(\,LCL_1 < Z_i < LCL_2)^c \\ + P(\,UCL_2 < Z_i \\ < UCL_1{}^{c})\}\{P(\,LCL_2 \le Z_i \le UCL_2)^c\}^i \end{aligned} \tag{5.16}$$

Then, Average Run Length of the process (ARL_1) that is not under control is:

$$ARL_1 = \frac{1}{1 - {P_{in}}^1} \tag{5.17}$$

Table 5.2 displays some of the comparison's observations between the new chart of monitoring a process suggested by Aslam et al.(2016) and to the chart developed by Saghir and Lin(2013).

Table 5.2: Comparison on Average Run Length values of Aslam et.al and Saghir and Lin's control charts when $\nu = 0.5$ and $ARL_0 = 500$

c	Aslam et.al λ=0.05	Saghir and Lin λ=0.05	Aslam et.al λ=0.20	Saghir and Lin λ=0.20
0.95	9.27	13.35	104.16	115.91
0.975	76.84	87.12	301.58	309.24
1	500	500	500	500
1.025	53.81	62.00	190.52	199.35
1.05	6.36	8.97	50.22	57.78

The results indicate that Aslam et al.'s method is faster in spotting shifts when the process is out-of-control compared to the other method and when λ is smaller is more sufficient than a larger value of λ according to the ARL_1 values.

5.3.2 Repetitive Sampling

A viable strategy for improving the efficacy of the GEWMA control chart is through repetitive sampling. The sampling technique known as repetitive sampling was initially introduced by Sherman (1965). Sherman claims that this sampling's operating process is similar to sequential sampling. This sstrategy has been employed frequently in the acceptance sampling plan field.

As before, two pairs of control limits will be used again. Step 1 is the same with MDS scheme as well as the declaration if the process is in-control or not. The difference now is that if none of them happens, start again to Step1 by resampling and repeat the process.

The pairs of the control limits are these that have been described in equations (5.12) and (5.13).

When the process is in a controlled state, the likelihood of declaring it as out of control based on a single sample, represented as $P^0_{out,1}$, can be expressed as:

https://doi.org/10.26219/heal.aueb.6224

$$P_{out,1}^{0} = P(Z_i < LCL_1) + P(Z_i > UCL_1) \tag{5.18}$$

The probability of recurrence, denoted as P_{rep}^{0}, in the event of the process being under control for the suggested control chart, may be expressed as follows.

$$P_{rep}^{0} = P(UCL_2 < Z_i < UCL_1) + P(LCL_1 < Z_i < LCL_2) \tag{5.19}$$

As a result, for the proposed control chart, the chance of declaring the process out of control while it is actually in control is calculated by:

$$P_{out}^{0} = \frac{P_{out,1}^{0}}{1 - P_{rep}^{0}} \tag{5.20}$$

In order to appraise the ARL in an out-of-control scenario, it is necessary to take into account the process shift. The parameter μ is altered to $\mu = c{*}\mu_0$, while maintaining a constant value for the parameter *v*, where *c* is a constant. The likelihood of announcing the out of control for the shifted process is given below:

$$P_{out,1}^{1} = P(Z_i < LCL_1 | \mu = c * \mu_0) + P(Z_i > UCL_1 | \mu = c * \mu_0) \tag{5.21}$$

The likelihood of resampling P_{rep}^{1}can be gotten similarly for the shifted process:

$$\begin{aligned} P_{rep}^{1} = {} & P(UCL_2 < T^* < UCL_1 | \mu = c * \mu_0) \\ & + P(LCL_1 < T^* < LCL_2 | \mu = c * \mu_0) \end{aligned} \tag{5.22}$$

The likelihood that the shifted process will declare itself to be out of control is thus given by:

$$P_{out}^{1} = \frac{P_{out,1}^{1}}{1 - P_{rep}^{1}} \tag{5.23}$$

As a result, the Average Run Length for the in-control and out-of-control are, respectively:

$$ARL_0 = \frac{1}{P_{out}^{0}} \tag{5.24}$$

$$ARL_1 = \frac{1}{P_{out}^{1}} \tag{5.25}$$

The mean sample size for the process under control, denoted as ASS_0 and the process with a shift, denoted as ASS_1 are indicated as follows:

$$ASS_0 = \frac{1}{1 - P_{rep}^{0}} \tag{5.26}$$

$$ASS_1 = \frac{1}{1 - P_{rep}^{1}} \tag{5.27}$$

The findings indicated a decrease in the Average Run Length values when comparing the control chart suggested by Saghir and Lin(2013) to the proposed control chart. It can thus be inferred that the proposed control chart is a more effective tool. This chart can identify by detecting instances where the process surpasses desired limits and deviates from standard specifications.

5.3.3 Use of a modified EWMA statistic

Khan et al.(2016) proposed a novel EWMA control chart that utilizes a modified EWMA statistic and accounts for historical data. The contemporary conduct of the mechanism and its present operational tendencies. The aforementioned concept may be effectively employed in the context of a first-order auto-correlated or independent normal sequence. In contrast to the usual EWMA statistic, a second parameter *k* is introduced to allow for the rapid detection of tiny process alterations. When compared to the traditional EWMA statistic, the modified EWMA statistic is able of detecting overall mean shift.

Given this as a stimulus, Aslam et al.(2017) introduced a novel control chart for the COM-Poisson distribution by employing this modified EWMA statistic which amalgamates the attributes of the EWMA technique and the difference between two recent observations.

Here are the steps to follow to create the chart that is suggested:

A sample of size *n* at time *i* is selected denoted as X_i . The modified EWMA statistic is calculated, represented as M_i.The recursive formula is the following:

$$M_i = (1 - \lambda)M_{i-1} + \lambda X_i + k(X_i - X_{i-1}) \tag{5.28}$$

where λ is the smoothing parameter, as always, and *k* is an accompanying constant associated to the technique.

The process is in-control if $LCL \leq M_i \leq UCL$, otherwise out-of-control.

According to Montgomery (2009), the range of λ in the interval [0.05,0.25] would be the best option for. The selection of the constant *k* can be made irrespective of λ. However, the results are based on $k = \frac{-\lambda}{2}$, that has been derived by Khan et al.(2016). This EWMA method is simplified to the conventional EWMA approach when *k* attains a value of zero.

The mean and the variance of the modified EWMA statistic M_i are shown below:

$$E(M_i) = \mu^{\frac{1}{\nu}} - \frac{\nu - 1}{2\nu} \tag{5.29}$$

https://doi.org/10.26219/heal.aueb.6224

$$Var(M_i) = \frac{(\lambda + 2\kappa\lambda + \kappa^2)}{2-\lambda}\left[\frac{\mu^{\frac{1}{\nu}}}{\nu}\right] \tag{5.30}$$

Subsequently, the upper control limit and the lower control limit are given as takes after:

$$UCL = \left(\mu_0 - \frac{\nu-1}{2\nu}\right) + L\sqrt{\frac{(\lambda + 2\kappa\lambda + \kappa^2)}{n(2-\lambda)}\left[\frac{\mu_0^{\frac{1}{\nu}}}{\nu}\right]} \tag{5.31}$$

$$LCL = \left(\mu_0^{\frac{1}{\nu}} - \frac{\nu-1}{2\nu}\right) - L\sqrt{\frac{(\lambda + 2\kappa\lambda + \kappa^2)}{n(2-\lambda)}\left[\frac{\mu_0^{\frac{1}{\nu}}}{\nu}\right]}$$

where μ_0 is the mean when the process is in-control and L, serves as a performance monitoring tool in the context of quality control. It should be noted that in the case where k is equal to zero, the limits become limited to Saghir and Lin(2013).

The results suggested that an escalation in the smoothing parameter λ elicits a proportional rise in the control chart multiplier L. Moreover, an increase in the value of λ causes a persistent depletion in the value at the first quartile.

The comparison between the modified EWMA chart and that of Saghir and Lin(2013) demonstrates that the former is more effective in detecting minimal to moderate deviations. To sum up, there is evidence to suggest that this method in question is superior in promptly detecting processes that are out of control when compared to other approaches in terms of Average Run Lengths.

5.4 A Hybrid EWMA

Haq (2013) suggested a hybrid model of EWMA control charts, which has since been referred to as the Hybrid EWMA control chart (HEWMA). The hybrid methodology under consideration comprises a customary EWMA chart that is incorporated with an unconventional EWMA chart.

The detection of minor and major shifts in the process mean is executed through a two-stage approach:

During the initial phase, the chart employs the conventional EWMA chart to detect minor changes in the process mean. In the event that a shift is detected by the standard EWMA chart, the chart transitions to its subsequent stage. In the succeeding stage, the chart transitions to the alternative EWMA chart characterized by the use of a dynamic smoothing parameter hinged on the sample standard deviation.

https://doi.org/10.26219/heal.aueb.6224

Aslam et.al(2016) extended this idea to a novel HEWMA, in which their statistical analysis is predicated upon a COM-Poisson distribution.

Let X be the number of non-conformities which follows a COM-Poisson distribution with parameters μ and ν. Let observations X_1,X_2... be independent and identically distributed random variables.

The recommended course of action for generating the proposed chart entails adherence to the following steps:

1. A random sample size of 1 is selected at time i, denoted as X_i . Then HEWMA statistic HE_i is calculated by using the recursive formula:

$$HE_i = \lambda_1 \cdot E_i + (1-\lambda_1) \cdot HE_{i-1} \tag{5.32}$$

where:

$$E_i = \lambda_2 \cdot X_i + (1-\lambda_2) \cdot E_{i-1} \tag{5.33}$$

In the two previous equations, λ_1 and λ_2 are two constants which take value in the interval (0,1]. It is worth noting that the suggested control chart can be simplified to EWMA chart that has been studied by Saghir and Lin(2013) when $\lambda_1 = 1$ and to Shewhart's when $\lambda_1 = \lambda_2 = 1$.

2. It is stated that the process is out-of-control when $HE_i \geq UCL \; or \; HE_i \leq LCL$ and in-control if $LCL \leq HE_i \leq UCL$.

Note that, E_i follows approximately the Normal distribution with mean and variance as described in Equations (5.9) and (5.10). Haq(2013) calculated the mean and the variance for the HE_i assuming that X_i also follows Normal distribution. The EWMA statistic has an impact of summing all past perceptions. Hence, it takes after that HE_i also follows approximately Normal distribution according to the Central Limit theory. The mean is equal to the one described in (5.9). As for the variance, it is calculated as:

$$Var(HE_i) = \frac{\lambda_1^2\lambda_2}{2-\lambda_2}\left[\frac{1-(1-\lambda_1)^{2i}}{\lambda_1(2-\lambda_1)} - \frac{(1-\lambda_2)^2\{(1-\lambda_2)^{2i}-(1-\lambda_1)^{2i}\}}{(1-\lambda_2)^2-(1-\lambda_1)^2}\right]\left[\frac{\mu^{\frac{1}{\nu}}}{\nu}\right] \tag{5.34}$$

Saghir and Lin(2013) recommended that when i is adequately large then the variance, when the process is in-control, is equal to:

$$Var(HE_i) = \frac{\lambda_1\lambda_2}{(2-\lambda_1)(2-\lambda_2)}\left[\frac{\mu_0^{\frac{1}{\nu}}}{\nu}\right] \tag{5.35}$$

Therefore, the control limits for this HEWMA chart are:

https://doi.org/10.26219/heal.aueb.6224

$$UCL = \left(\mu_0{}^{\frac{1}{\nu}} - \frac{\nu - 1}{2\nu} \right) + L \sqrt{\frac{\lambda_1 \lambda_2}{(2-\lambda_1)(2-\lambda_2)} \left[\frac{\mu_0{}^{\frac{1}{\nu}}}{\nu} \right]} \qquad (5.36)$$

$$LCL = \left(\mu_0{}^{\frac{1}{\nu}} - \frac{\nu - 1}{2\nu} \right) - L \sqrt{\frac{\lambda_1 \lambda_2}{(2-\lambda_1)(2-\lambda_2)} \left[\frac{\mu_0{}^{\frac{1}{\nu}}}{\nu} \right]}$$

When the process is in a controlled state, the likelihood of declaring it as out of control represented as P_{out}^{0} , can be computed as:

$$P_{out}^{0} = P(HE_i \leq LCL|\mu_0) + P(HE_i \geq UCL|\mu_0) \qquad (5.37)$$

The likelihood of being declared as out of control for the shifted process is given below:

$$P_{out}^{1} = P(HE_i < LCL|\mu = c * \mu_0) + P(HE_i > UCL|\mu = c * \mu_0) \qquad (5.38)$$

As a result, the Average Run Lengths are derived as:

$$ARL_0 = \frac{1}{P_{out}^{0}} \qquad (5.39)$$

$$ARL_1 = \frac{1}{P_{out}^{1}} \qquad (5.40)$$

The simulation results show that the values of ARL_1 manifest a swift reduction as the value of c declines or ascends. The decline in the values of ARL_1 is more substantial with an increase in the value of *c*, as opposed to a decrease in its value. It is also observed that the ARL_1 diminishes in magnitude with a corresponding decrease in λ_2.

5.5 Double EWMA control chart for CMP data

Numerous schemes have been devised for the EWMA chart to enhance its sensitivity in detecting minute variations in a given process. Shamma et al.(1991) and Shamma and Shamma(1992) presented a novel approach in statistical process control referred to as the Double EWMA (DEWMA), and it was proposed for the purpose of monitoring normally distributed data. Later, Zhang et al.(2003) expand on this concept to produce a new chart, the DEWMA for Poisson distributed data.

This idea was expanded also for the COM-Poisson attributes by Alevizakos and Koukouvinos(2019) who created a new DEWMA control chart based on these observations, denoted as CMP-DEWMA.

https://doi.org/10.26219/heal.aueb.6224

The suggested chart is researched to detect shifts in both parameters simultaneously as well as shifts in each parameter individually, unlike all prior EWMA control charts based on the COM-Poisson distribution, which were only studied for monitoring shifts for one parameter. In other words, their aim is to do the analysis of changes in the location parameter μ while keeping the value of ν constant, alterations in the dispersion parameter ν while keeping the value of μ constant, as well as adjustments in both parameters simultaneously.

Let $X_i \sim CMP(\mu, \nu)$ independent and identically distributed random variables.When the process is in control μ=μ_0 and $\nu = \nu_0$.

The CMP-DEWMA statistic is defined by the system of the following equations:

$$Z_i = \lambda \cdot X_i + (1-\lambda) \cdot Z_{i-1} \tag{5.41}$$

$$Y_i = \lambda \cdot Z_i + (1-\lambda) \cdot Y_{i-1}$$

$$Z_0 = Y_0 = \mu_0 \frac{\partial \log(z(\mu_0, \nu_0))}{\partial \mu_0}$$

The mean and the variance of Y_i , when the process is in-control, are given as:

$$E(Y_i) = \mu_0 \frac{\partial \log(z(\mu_0, \nu_0))}{\partial \mu_0} \tag{5.42}$$

$$Var(Y_i) = \frac{\begin{array}{c}\lambda^4[1+(1-\lambda)^2 - (i+1)^2(1-\lambda)^{2i} \\ +(2i^2+2i-1)(1-\lambda)^{2i+2} - i^2(1-\lambda)^{2i+4}]\end{array}}{[1-(1-\lambda)^2]^3} \frac{\partial E(X)}{\partial \mu_0} \tag{5.43}$$

The control limits are:

$$UCL_i = \mu_0 \frac{\partial \log(z(\mu_0, \nu_0))}{\partial \mu_0} + L\sqrt{Var(Y_i)} \tag{5.44}$$

$$Center\ Line = \mu_0 \frac{\partial \log(z(\mu_0, \nu_0))}{\partial \mu_0}$$

$$LCL_i = \mu_0 \frac{\partial \log(z(\mu_0, \nu_0))}{\partial \mu_0} - L\sqrt{Var(Y_i)}$$

As *i* increases, the control limits described in Equation (5.44) converge to :

$$UCL = \mu_0 \frac{\partial \log(z(\mu_0, \nu_0))}{\partial \mu_0} + L \sqrt{\frac{\frac{\partial E(X)}{\partial \mu_0} \lambda [2 - 2\lambda + \lambda^2]}{(2-\lambda)^3}} \tag{5.45}$$

https://doi.org/10.26219/heal.aueb.6224

$$Center\ Line = \mu_0 \frac{\partial \log(z(\mu_0 , \nu_0))}{\partial \mu_0}$$

$$LCL = \mu_0 \frac{\partial \log(z(\mu_0 , \nu_0))}{\partial \mu_0} - \ L \sqrt{\frac{\frac{\partial E(X)}{\partial \mu_0}\ \lambda\,[2 - 2\lambda + \lambda^2]}{(2-\lambda)^3}}$$

Note that, if the computed value is less than zero, *LCL* is set to zero.

Next up, a comparison between the Saghir and Lin(2013) and Alevizakos and Koukouvinos(2019). The findings of the performance analysis indicated that the CMP-DEWMA chart demonstrated significant utility. The Saghir and Lin's chart is surpassed in performance by the proposed methodology in instances where there are downward shifts in the location parameter, at a fixed level of the dispersion parameter, as well as when there are upward shifts in the dispersion parameter, under a fixed value of the location parameter. In addition, the proposed methodology is superior to the Saghir and Lin's chart when there are concurrent upward shifts and downward shifts in the parameters that are indicative of a decrease in the mean value of the process.

 https://doi.org/10.26219/heal.aueb.6224

Chapter 6

Simulation Study

Statistical Quality Control has the potential to make a significant contribution to the domain of health surveillance. In the realm of this, it is common to monitor and evaluate infrequent health occurrences, such as epidemics, adversarial responses to pharmaceutical treatments, or exceptional negative effects within clinical trials. The Poisson distribution is frequently employed as a means of modeling the incidence of infrequent occurrences, owing to its applicability to count data characterized by independent and constant-rate events. For example, in the context of monitoring adverse events that may arise from medication use, it is imperative to discern both increases and decreases in such events, which may indicate potential safety concerns and effectiveness issues, respectively.

In the present chapter, a simulation study was conducted to appraise the efficiency of some EWMA control charts for Poisson observations, which have been described in Chapter 3. The goal is to provide a more extensive comparative analysis of the two sided PTEWMA by Alevizakos et al.(2022), PDEWMA by Zhang et al.(2003) and PEWMA by Borror et al.(1998) regarding the values of λ, inspired by the research of Alevizakos et al. (2022) on Triple Poisson EWMA control charts. The results of the comparison and the simulation methology are presented below.

6.1 Simulation procedure

A Monte Carlo simulation was employed in the implementation of all these three types of control charts. The Monte Carlo simulation is an analytical procedure that utilizes stochastic sampling and probability theory for modeling and examining intricate systems or processes. The methodology entails conducting iterative simulations through the utilization of stochastic inputs as a means of approximating the potential outcomes and their likelihoods.

A total of 20.000 datasets, each comprised of 20.000 random variables following a Poisson distribution with parameter μ_0, were simulated. The dataset of each simulation was generated using *rpois* function in R.

After specifying a value of ARL_0 as 370, the optimal L for each of the desirable values of λ has been calculated. The utilization of the value 370 can be attributed to the fact that α corresponds to the likelihood of a single point surpassing the bounds in a state of in control, with a value of 0.0027, and ARL_0 is derived from dividing one by α.

Upon defining the values of λ and L, an analysis is conducted wherein the charting statistics for each of the control charts and control limits are computed. If the resulting

 https://doi.org/10.26219/heal.aueb.6224

statistic falls within the bounds of the lower control limit and upper control limit it is regarded as being in control. Any statistic that falls outside of these limits signifies the process as being out of control thereby necessitating a cessation of the simulations and the recording of the run-length.

After determining the most advantageous L value to attain ARL_0 370, an investigation ensues as to whether or not a processing modification will promptly reflect upon the control charts. A dataset consisting of 20,000 randomly generated variables following a Poisson distribution was simulated repeatedly, resulting in the generation of 20,000 new datasets. Each of these newly simulated datasets was characterized by a distinct parameter μ_1, calculated as $\mu_0 + d * \sigma$, where d represents the magnitude of the shift to be added or subtracted and σ is equal to $\sqrt{\mu_0}$, due to Poisson distribution. Then, ARL_1 values have been calculated and compared for each combination of λ and μ_1.

6.2 Measures of evaluation

The determination of the ARL in a control chart context is dependent upon the examination of two distinct states: the zero-state ARL values and the steady-state ARL values. The former is derived from sustained shifts in the parameter that are observed under the initial startup conditions of the control chart, while the latter is obtained through the detection of delayed shifts in the parameter.

In the present study, the assessment of performance shall be conducted utilizing the time-varying control limits and steady state Average Run Length values. This methodology is particularly applicable when the process in question is susceptible to encountering shifts or trends over time; hence, the primary concern is to efficiently detect and respond to such changes in a prompt manner. The implementation of time-varying control limits is conducive to a higher degree of sensitivity with regard to process shifts. Complementary to this, steady state analysis provides a means of evaluating the average run under conditions of stability.

The utilization of fixed control limits in combination with a zero state is deemed suitable under circumstances where the process is anticipated to retain a state of stability and demonstrate negligible variations over time. The establishment of control limits that are fixed is dependent upon either historical data or specifications. This procedure is premised on the assumption that the process observed is in a condition of statistical control. The zero state denotes the absence of any anticipated systematic shifts or trends.

So, for the comparison of these control charts we will assume that the process is in a state of in control. Therefore, the measures of performance will be steady-state ARL values and the Standard Deviation of them.

https://doi.org/10.26219/heal.aueb.6224

6.3 Performance

The effectiveness of the PEWMA, PDEWMA, and PTEWMA control charts was assessed. The present research delves into the analysis of the run-length distribution of the suggested charts, exploring their in control design, along with its performance in the steady-state out of control state. The methodology for the in-control design was explicated in Subchapter 6.1 .To address the issue of out of control performance, three discrete levels of shifts were incorporated: a minor magnitude change, a moderate magnitude change, and a major magnitude change.

When comparing control charts, it is imperative to acknowledge the various types of alterations that might arise in the monitored process. When comparing control charts, it is important to consider different types of changes that may occur in the process being monitored. This includes small, medium, and big changes. Through the discerning analysis of the efficacy of control charts in relation to diverse forms of alterations, significant patterns can be revealed, the resilience of each chart can be evaluated, and crucial comparisons can be made. It is imperative to ensure that the selected control chart has the capability to detect slight, moderate, and significant alterations, given that the significance of such changes can differ based on contextual factors and specific monitoring requisites associated with the process.

The presented tables offer significant elucidations regarding the proficient performance of the aforementioned control charts. Moreover, they provide a comprehensive analysis of the charts' capabilities to identify and react to shifts of diverse magnitudes in the process mean.

6.3.1 In control performance

Some of the findings derived from control charts are presented in Tables 6.1 to 6.3, which incorporate various mean values of 4, 8, and 12 and λ values between [0.1,0.9]. The present study refrains from utilizing the λ value of 1 in the EWMA control charts, owing to the fact that, at this specific value, the charts are indistinguishable from the Shewhart control charts.

Employing different means for the Poisson distribution whilst contrasting control charts enables the appraisal of the efficacy of each chart in varying situations or contexts. This statement elucidates the utility of evaluating the capacity of each graphic illustration to detect and react to fluctuations in the average parameter of the scrutinized procedure. Therefore, the mean values of 4, 8 and 12 are given.

Generally, the determination of the optimal value for the smoothing parameter λ necessitates the attainment of an appropriate trade-off between the ability to adequately detect process shifts and the mitigation of the impact of extraneous variation. A reduction in the value of λ enhances the sensitivity, but this outcome may

https://doi.org/10.26219/heal.aueb.6224

augment both the incidence of false alarms and the extent of noise. In contrast, the use of a larger value of λ may diminish noise levels. However, it may also prolong the process of detecting genuine shifts. When considering the optimization of processes, several factors should be taken into account. These factors include, but are not limited to, the variability and magnitude of process shifts, an analysis of historical data, the utilization of trial and error methodologies, the identification and balancing of the trade-off between responsiveness and detection delay, and the incorporation of domain expertise. In essence, determining the optimal smoothing parameter necessitates a meticulous assessment and fine-tuning tailored to the distinctive attributes and exigencies of the given process.

The following Tables 6.1 through 6.3, display information pertaining to L values (sideways) required to obtain a specified ARL_0 value of 370. The aforementioned tables also provide the ARL_0 as well as $SDRL_0$values, enclosed in parentheses, for the three different control charts, PEWMA, PDEWMA, and PTWEMA respectively.

Table 6.1: Values of L for the PEWMA control chart to achieve $ARL_0 \approx 370$

λ	**PEWMA** ($\mu_0 = 4$)	**PEWMA** ($\mu_0 = 8$)	**PEWMA** ($\mu_0 = 12$)
0.1	*2.723* 370.994 (382.2617)	*2.719* 370.2573 (384.3862)	*2.714* 370.7337 (378.1754)
0.2	*2.891* 370.5671 (373.6116)	*2.879* 369.7474 (376.2424)	*2.872* 370.9637 (372.805)
0.3	*2.994* 370.6455 (376.6385)	*2.958* 370.2215 (372.8777)	*2.945* 370.2371 (373.2787)
0.4	*3.067* 370.0533 (370.4406)	*3.011* 370.2346 (372.2239)	*2.990* 370.3181 (374.7152)
0.5	*3.134* 369.3954 (370.8073)	*3.049* 370.3023 (377.316)	*3.025* 370.848 (372.8020)
0.6	*3.190* 369.9991 (371.1867)	*3.083* 370.0281 (373.2359)	*3.051* 370.0376 (368.035)
0.7	*3.235*	*3.112*	*3.068*

https://doi.org/10.26219/heal.aueb.6224

	370.1302 (371.474)	370.5657 (373.6906)	370.3947 (368.349)
0.8	*3.270* 369.2647 (366.0396)	*3.133* 370.2155 (373.3968)	*3.081* 370.2377 (369.2863)
0.9	*3.337* 369.5539 (367.0377)	*3.157* 370.3942 (375.0640)	*3.097* 370.5472 (368.8260)

Table 6.2: Values of L for the PDEWMA control chart to achieve $ARL_0 \approx 370$

λ	**PDEWMA ($\mu_0 = 4$)**	**PDEWMA ($\mu_0 = 8$)**	**PDEWMA ($\mu_0 = 12$)**
0.1	*2.240* 370.3734 (389.1349)	*2.244* 370.0842 (390.578)	*2.245* 369.6156 (390.0875)
0.2	*2.534* 370.5812 (381.9925)	*2.533* 370.2721 (381.8238)	*2.533* 370.1351 (381.0375)
0.3	*2.703* 370.0573 (376.5039)	*2.705* 370.9824 (377.8323)	*2.698* 370.1435 (375.2457)
0.4	*2.825* 370.3675 (371.2442)	*2.822* 370.5041 (374.2491)	*2.816* 370.8853 (369.6306)
0.5	*2.921* 370.4441 (375.6602)	*2.905* 370.2496 (371.6294)	*2.898* 370.2543 (375.0982)
0.6	*3.017* 370.8757 (368.6222)	*2.976* 370.8093 (371.2482)	*2.964* 370.6998 (373.9438)
0.7	*3.112* 370.83 (373.5394)	*3.035* 370.7525 (375.1697)	*3.013* 370.8283 (372.8801)

 https://doi.org/10.26219/heal.aueb.6224

0.8	*3.201* 370.7813 (370.1632)	*3.086* 370.0866 (372.5761)	*3.055* 370.43 (369.6825)
0.9	*3.269* 370.2376 (366.6146)	*3.134* 370.0961 (373.5072)	*3.072* 370.5283 (370.1320)

Table 6.3: Values of L for the PDEWMA control chart to achieve $ARL_0 \approx 370$

λ	PTEWMA ($\mu_0 = 4$)	PTEWMA ($\mu_0 = 8$)	PTEWMA ($\mu_0 = 12$)
0.1	*2.047* 370.3913 (394.5347)	*2.053* 370.3413 (401.9395)	*2.045* 370.3592 (396.2641)
0.2	*2.356* 370.5270 (380.8544)	*2.358* 370.6656 (384.0903)	*2.353* 370.0951 (378.5654)
0.3	*2.535* 370.6939 (378.9661)	*2.536* 370.2222 (380.8053)	*2.534* 370.0118 (377.7093)
0.4	*2.675* 370.1270 (376.2339)	*2.675* 370.1992 (378.5222)	*2.669* 370.3143 *(373.3306)*
0.5	*2.792* 370.3763 (370.6737)	*2.787* 369.8512 (372.4572)	*2.784* 370.6266 (369.2474)
0.6	*2.895* 370.5944 (370.7401)	*2.881* 370.0212 (373.6245)	*2.875* 369.8005 (372.0287)
0.7	*2.998* 370.5454 (372.1636)	*2.964* 370.1692 (371.1107)	*2.953* 370.4231 (373.0624)
0.8	*3.121* 370.9202	*3.049* 369.9699	*3.017* 369.981

 https://doi.org/10.26219/heal.aueb.6224

	(375.0731)	(375.3566)	(371.7389)
0.9	*3.240* 370.2074 (368.9052)	*3.114* 370.3822 (372.6542)	*3.069* 369.6845 (368.6136)

It can be observed that, as λ increases in magnitude in all three control charts, there is a corresponding increase in the corresponding L value. It is noteworthy that, in the context of control charts, as the value of λ remains constant and μ is subsequently varied from 4 to 8 and then to 12, the value of L is relatively stable with slight fluctuations but the differences in L values are increasing as λ increases. Furthermore, it can be observed that an increase in λ yields a concomitant increase in the standard deviation of the run length across all three control charts.

Figure 6.1 illustrates the outcomes of the L values pertaining to each of the control charts under the condition of $\mu_0 = 4$.

Figure 6.1: Comparison of L values in all three control charts when $\mu_0 = 4$

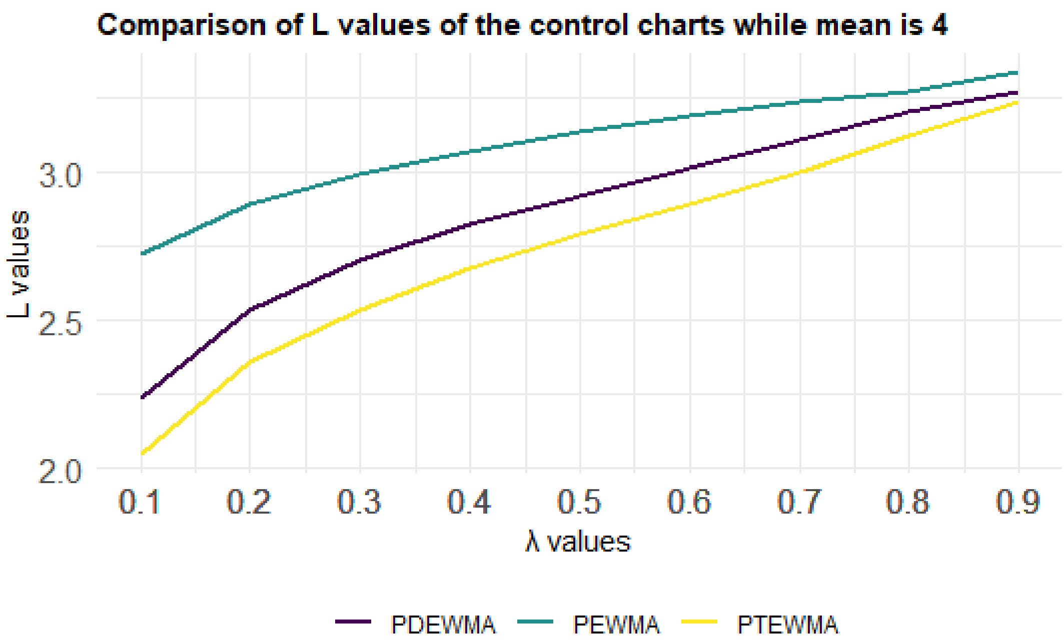

It can be observed that, as λ increases in magnitude in all three control charts, there is a corresponding increase in the corresponding L value. An intriguing finding one can see also in the previous tables, is that, when the values of μ and λ remain constant, the level of L appears to be the lowest in the case of PTEWMA, increased in PDEWMA, and further increased in PEWMA. The identical outcomes to those obtained in this figure are likewise observed when the mean value assumes the values of 8 and 12.

https://doi.org/10.26219/heal.aueb.6224

It is imperative to acknowledge that there may be fluctuations in the outcomes in relation to the findings presented in the study conducted by Alevizakos et al.(2022). The possible reason for this occurrence could be attributed to the disparate amounts of repetitions performed, with the former featuring 50.000 and the latter bearing 20.000, as outlined here. However, it should be noted that they exhibit a degree of consistency.

6.3.2 Out of control performance

As it has been previously said, upon identifying the optimal value of L for every λ and μ combination, a total of 20,000 datasets were generated. These datasets comprised 20,000 randomly generated variables derived from a Poisson distribution characterized by a mean value of μ_1, which is equal to $\mu_0 + d * \sqrt{\mu_0}$.

The determination of the particular parameters of d associated with various degrees of alteration (e. g, small, medium, or large) within a Poisson distribution is contingent upon contextual factors and the intended magnitude of significance or threshold. The categorization of a modification as being insignificant, moderate, or significant is reliant on personal interpretation and may fluctuate based on the precise usage or established standards within a given industrial setting. It is noteworthy to acknowledge that the values of the coefficient *d* alongside the classification of changes as small, medium, and big, may exhibit variability contingent upon the distinctive needs and established norms of the given application or industry.

In the realm of monitoring undesired events associated with medication utilization, the delineation of noteworthy alterations can be influenced by a multitude of factors, including regulatory protocols, safety thresholds, and the specific characteristics of the undesirable outcomes under scrutiny. From a broader perspective:

The concept of small change pertains to a scenario wherein there exists a marginal hike or decline in unfavorable occurrences. This phenomenon can be deemed applicable in instances where the mean experiences a relatively inconsequential shift.. A change of moderate magnitude may become pertinent when there is a significant upsurge or deduction in deleterious occurrences. The abovementioned observation may indicate a movement of approximately 1 to 2 standard deviations away from the initial mean, signifying a notable alteration. Finally, a major alteration can be defined as a transition exceeding two standard deviations from the initial mean.

The incremental modifications of minimal magnitude, in both positive and negative shifts, shall be denoted by the values of *d*, specifically 0.05, 0.25, and 0.5 This designation is preferred as all control charts possess the ability to detect process deviation from the norm. However, it is of greater interest to observe if a process is experiencing slight variations. Such minor changes may signify the onset of potential deviations or complications in the process, thus serving as a preemptive indicator. By

 https://doi.org/10.26219/heal.aueb.6224

promptly identifying and addressing subtle alterations, it is feasible to preclude their escalation into consequential and complex predicaments.

The current set of Tables 6.4 through 6.6 presents data relevant to the ARL_1 values for the three control charts, with respect to certain alterations in the mean under mean values of 4, 8, and 12.

Therefore, if the mean value is equal to 4, the resultant new mean μ_1 is anticipated to assume any of the following values: 3, 3.5, 3.9, 4.1, 4.5 and 5. When the mean of a set of data is equal to 8, the resulting new mean μ_1 will take on the values of 6.59, 7.29, 7.86, 8.14, 8.71, and 9.41. At a mean value of 12, the resulting means μ_1 are observed to be 10.27, 11.13, 11.83, 12.17, 12.87 and 13.73.

The ARL_1 values of the three control charts exhibit significant differences, and the presence of decimal points does not impede their interpretation. Therefore, in consideration of the need for ease of comprehension and appearance, numerical values were subjected to rounding.

Table 6.4: ARL_1 values from the comparison of the three control charts in shifts while process mean $\mu_0 = 4$

λ	d	PEWMA ($\mu_0 = 4$)	PDEWMA ($\mu_0 = 4$)	PTEWMA ($\mu_0 = 4$)
0.1	-0.5	30	$\boxed{22}$	$\boxed{22}$
	-0.25	120	73	$\boxed{68}$
	-0.05	408	336	$\boxed{324}$
	0.05	$\boxed{275}$	290	291
	0.25	70	65	$\boxed{63}$
	0.5	23	$\boxed{21}$	22
0.2	-0.5	61	29	$\boxed{26}$
	-0.25	287	115	$\boxed{94}$
	-0.05	468	387	$\boxed{366}$
	0.05	$\boxed{270}$	290	294
	0.25	81	78	$\boxed{74}$
	0.5	28	25	$\boxed{24}$
0.3	-0.5	157	42	$\boxed{33}$
	-0.25	679	180	$\boxed{134}$
	-0.05	495	420	$\boxed{393}$
	0.05	$\boxed{273}$	288	298
	0.25	90	85	$\boxed{82}$
	0.5	32	28	$\boxed{27}$
0.4	-0.5	628	69	$\boxed{45}$
	-0.25	1353	291	$\boxed{191}$
	-0.05	495	450	$\boxed{420}$
	0.05	$\boxed{279}$	285	291
	0.25	102	91	$\boxed{88}$
	0.5	38	31	$\boxed{29}$

 https://doi.org/10.26219/heal.aueb.6224

0.5	-0.5	4554	135	$\boxed{70}$
	-0.25	1630	526	$\boxed{288}$
	-0.05	484	472	$\boxed{446}$
	0.05	284	$\boxed{281}$	287
	0.25	111	95	$\boxed{94}$
	0.5	43	34	$\boxed{32}$
0.6	-0.5	7554	425	$\boxed{129}$
	-0.25	1454	1059	$\boxed{489}$
	-0.05	475	491	$\boxed{468}$
	0.05	290	$\boxed{282}$	285
	0.25	122	102	$\boxed{98}$
	0.5	50	38	$\boxed{35}$
0.7	-0.5	6053	3340	$\boxed{338}$
	-0.25	1303	1585	$\boxed{980}$
	-0.05	$\boxed{475}$	487	484
	0.05	295	287	$\boxed{282}$
	0.25	133	114	$\boxed{103}$
	0.5	57	44	$\boxed{39}$
0.8	-0.5	$\boxed{4835}$	6826	5396
	-0.25	$\boxed{1176}$	1385	1576
	-0.05	$\boxed{466}$	472	481
	0.05	300	294	$\boxed{288}$
	0.25	142	128	$\boxed{117}$
	0.5	64	53	$\boxed{46}$
0.9	-0.5	$\boxed{3906}$	4700	5631
	-0.25	$\boxed{1068}$	1164	1270
	-0.05	$\boxed{449}$	456	464
	0.05	307	301	$\boxed{298}$
	0.25	154	143	$\boxed{137}$
	0.5	74	65	$\boxed{59}$

Table 6.5: ARL_1 values from the comparison of the three control charts in shifts while process mean $\mu_0 = 8$

λ	d	PEWMA ($\mu_0 = 8$)	PDEWMA ($\mu_0 = 8$)	PTEWMA ($\mu_0 = 8$)
0.1	-0.5	29	$\boxed{21}$	22
	-0.25	107	70	$\boxed{66}$
	-0.05	380	$\boxed{317}$	318
	0.05	$\boxed{289}$	299	297
	0.25	73	66	$\boxed{62}$
	0.5	24	22	$\boxed{22}$
0.2	-0.5	49	28	$\boxed{26}$
	-0.25	201	107	$\boxed{91}$
	-0.05	423	366	$\boxed{356}$
	0.05	$\boxed{287}$	298	304
	0.25		81	

https://doi.org/10.26219/heal.aueb.6224

	0.5	88 29	25	$\boxed{76}$ $\boxed{24}$
0.3	-0.5 -0.25 -0.05 0.05 0.25 0.5	88 348 452 $\boxed{289}$ 99 34	38 153 392 301 90 29	$\boxed{31}$ $\boxed{121}$ $\boxed{372}$ 302 $\boxed{86}$ $\boxed{27}$
0.4	-0.5 -0.25 -0.05 0.05 0.25 0.5	171 558 463 $\boxed{290}$ 109 40	55 218 416 301 99 33	$\boxed{41}$ $\boxed{162}$ $\boxed{393}$ 304 $\boxed{94}$ $\boxed{30}$
0.5	-0.5 -0.25 -0.05 0.05 0.25 0.5	356 807 464 $\boxed{292}$ 118 45	86 319 434 296 106 37	$\boxed{56}$ $\boxed{218}$ $\boxed{413}$ 303 $\boxed{102}$ $\boxed{33}$
0.6	-0.5 -0.25 -0.05 0.05 0.25 0.5	768 1006 462 296 126 51	152 476 441 $\boxed{292}$ 112 41	$\boxed{85}$ $\boxed{308}$ $\boxed{429}$ 299 $\boxed{109}$ $\boxed{37}$
0.7	-0.5 -0.25 -0.05 0.05 0.25 0.5	1634 1097 461 299 136 57	342 757 461 $\boxed{293}$ 121 46	153 472 445 297 $\boxed{115}$ $\boxed{42}$
0.8	-0.5 -0.25 -0.05 0.05 0.25 0.5	2082 1095 455 302 146 64	999 1018 459 $\boxed{297}$ 131 54	418 830 472 301 $\boxed{125}$ $\boxed{49}$
0.9	-0.5 -0.25 -0.05 0.05 0.25 0.5	3657 $\boxed{1065}$ $\boxed{452}$ 305 153 71	2855 1090 455 303 147 65	$\boxed{1878}$ 1082 457 $\boxed{300}$ $\boxed{139}$ $\boxed{60}$

https://doi.org/10.26219/heal.aueb.6224

Table 6.6: ARL_1 values from the comparison of the three control charts in shifts while process mean $\mu_0 = 12$

λ	d	PEWMA ($\mu_0 = 12$)	PDEWMA ($\mu_0 = 12$)	PTEWMA ($\mu_0 = 12$)
0.1	-0.5	28	$\boxed{22}$	$\boxed{22}$
	-0.25	101	71	$\boxed{66}$
	-0.05	371	329	$\boxed{316}$
	0.05	$\boxed{295}$	298	295
	0.25	76	65	$\boxed{63}$
	0.5	24	$\boxed{21}$	22
0.2	-0.5	45	28	$\boxed{25}$
	-0.25	178	103	$\boxed{89}$
	-0.05	408	359	$\boxed{350}$
	0.05	$\boxed{297}$	305	306
	0.25	93	82	$\boxed{77}$
	0.5	30	25	$\boxed{24}$
0.3	-0.5	75	37	$\boxed{31}$
	-0.25	279	143	$\boxed{116}$
	-0.05	427	382	$\boxed{365}$
	0.05	$\boxed{297}$	310	307
	0.25	104	95	$\boxed{89}$
	0.5	35	29	$\boxed{27}$
0.4	-0.5	125	52	$\boxed{39}$
	-0.25	409	197	$\boxed{151}$
	-0.05	437	408	$\boxed{383}$
	0.05	$\boxed{297}$	309	310
	0.25	114	105	$\boxed{99}$
	0.5	41	33	$\boxed{30}$
0.5	-0.5	216	76	$\boxed{53}$
	-0.25	566	270	$\boxed{198}$
	-0.05	451	422	$\boxed{406}$
	0.05	$\boxed{301}$	306	310
	0.25	124	112	$\boxed{108}$
	0.5	48	38	$\boxed{34}$
0.6	-0.5	368	120	$\boxed{76}$
	-0.25	710	381	$\boxed{264}$
	-0.05	453	433	$\boxed{417}$
	0.05	$\boxed{305}$	307	310
	0.25	133	120	$\boxed{114}$
	0.5	54	43	$\boxed{39}$
0.7	-0.5	607	215	$\boxed{121}$
	-0.25	801	540	$\boxed{373}$
	-0.05	450	442	$\boxed{430}$
	0.05	305	$\boxed{301}$	308
	0.25	141	128	$\boxed{122}$
	0.5	61	49	$\boxed{44}$

 https://doi.org/10.26219/heal.aueb.6224

0.8	-0.5	936	449	$\boxed{243}$
	-0.25	854	740	$\boxed{569}$
	-0.05	445	449	$\boxed{443}$
	0.05	306	307	$\boxed{300}$
	0.25	148	138	$\boxed{130}$
	0.5	68	58	$\boxed{51}$
0.9	-0.5	1430	921	$\boxed{682}$
	-0.25	877	827	$\boxed{812}$
	-0.05	441	$\boxed{433}$	445
	0.05	308	$\boxed{300}$	305
	0.25	156	146	$\boxed{144}$
	0.5	75	67	$\boxed{63}$

Initially, it must be noted that our focus lies upon the minimum ARL_1 value. This value denotes the anticipated number of samples prior to a control chart indicating an out-of-control process. It is particularly significant as it reflects a swift manifestation of a shift in the process.

Here are some comments regarding the performance of each control chart:

- Triple Poisson EWMA (PTEWMA)

In every combination of the parameters λ and μ, it has been observed that an increase in mean is demonstrated relatively quicker compared to a decrease. In the tables of the PTEWMA, it is evident that as the positive *d*-value increases (indicating a larger magnitude of change), and similarly when the negative *d*-value increases in absolute terms (indicating also a larger magnitude of change), the ARL_1 of the PTEWMA for detecting change decreases, signifying a faster identification of change. However, in a minority of cases, it is notable that the disparity between *d*=-0. 025 and -0.05 or *d* =-0.5 and -0.25 is considerable. Should the ARL_1value be greater for a shift of larger magnitude (-0. 25) as opposed to a smaller shift (-0.05), it may signify a reduction in sensitivity of the control chart when it comes to identifying greater shifts in the process. There may be several factors contributing to this phenomenon, including inherent process variability or deficiencies in the control chart's design. The intrinsic variability of the process is pivotal in determining the sensitivity of the control chart. In situations where a process displays high variability, a greater degree of deviation may be necessary to surpass established control limits and prompt the detection of anomalies, thereby generating a prolonged ARL_1.

In the domain of control chart design, if the control chart is configured with lower sensitivity or wider control limits, it would necessitate a considerable shift to elicit detection, resulting in an elevated ARL_1 value for larger shifts. Finally, under a constant λ, in instances where the mean fluctuates between 4 to 8 and 8 to 12 with a

https://doi.org/10.26219/heal.aueb.6224

positive *d*, the ARL_1 value remains relatively consistent. Nonetheless, in identical conditions, while *d* is negative, the ARL_1 parameter experiences a significant decline.

- Poisson EWMA (PEWMA)

For every pairing of λ and μ, the positive changes are discerned more rapidly in contrast to the negative changes. When constant λ and *d*=+0.05, the ARL_1 value exhibits an increasing trend when μ varies from 4 to 8 and 8 to 12. However, when changes in +0.25 and +0.5 occur, the ARL_1 value remains relatively stable despite an increase in μ. Once again, as before in the PTEWMA, in a minority of cases, it is notable that the disparity between *d*=-0. 025 and -0.05 or *d* =-0.5 and -0.25 is significant and the possible reasons were described before. A notable discovery reveals that the ARL_1 can reach stabilization when the value of λ is set to 0.7, 0.8 or 0.9 in conjunction with a seemingly small value of *d* equaling +0.05. As the constant value of μ is held, an increase in λ is associated with a consistent and upward trend in the ARL_1. This phenomenon can be attributed to the representation of λ as a measure of the weight assigned to new incoming observations. Under circumstances where the new observation exhibits a change, the control chart becomes cognizant of this update in a delayed manner. Last but not least, in the Tables 6.4 to 6.6, extreme values of ARL_1 are observed such as 7554. This implies that the control chart is not performing optimally and needs further improvement.

- Double Poisson EWMA (PDEWMA)

As PEWMA and PTEWMA, for each matching of λ and μ, the positive changes are observed more quickly in differentiate to the negative changes. As from the PDEWMA table, as in the other two control diagrams, it is clear that the ARL_1 of the PDEWMA for detecting changes decreases with the increase of positive d values (which also indicate greater changes), as does the negative d values in absolute terms (which also indicate greater changes), indicating a faster identification of changes. However, in a few cases, the differences between d=-0.025 and -0.05 or d=-0.5 and -0.25 are considerable. In any case, when consistent λ, and μ shifts from 4 to 8 and 8 to 12, in positive changes, the ARL_1 has an increasing trend instead of steady as PEWMA with *d*=+0.05. In addition also for the PDEWMA, extreme values are observed and needs further improvement too.

From the comparison of the control charts the results indicate that:

Irrespective of the value of μ, it has been observed that for smaller values of λ and d equal to +0.05, the PEWMA is more effective. For the same value of positive *d*, the PDEWMA control chart appears to perform superiorly when utilizing a medium value of λ. For higher magnitudes of λ, PTEWMA exhibits superior performance when compared to the other two. The PTEWMA has displayed superior performance compared to the others when the value of *d* assumes the values of +0.25 and +0.50, exhibiting notable differences in some scenarios. For the negative value of *d*, it is clear that the PTEWMA outperforms the other control charts in each case of change.

 https://doi.org/10.26219/heal.aueb.6224

Even when the PDEWMA has a smaller ARL_1, the values with PTEWMA are very close.

Finally, the comparative analysis demonstrated the findings for various combinations of λ and μ.The study was concentrated on minor changes because they are the most significant for a process, and chose positive and negative changes of 0.05, 0.25, and 0.5 standard deviations. When the main interest is on positive change in the mean, the PTEWMA control chart must be utilized. When the focus is on negative change, the magnitude is what we are interested in. One thing to keep in mind is that none of these control charts have significantly better performance, and the ARL_1 values are rather close for the positive changes. On the other hand for the negative changes and as λ increase the PEWMA and PDEWMA seem to have a significant issue. As a conclusion, in order to decide which of the three we should use to detect the change more rapidly, it must be carefully considered the mean, the shift, and the weighting parameter.

https://doi.org/10.26219/heal.aueb.6224

Chapter 7

Conclusions and Further Research

In this thesis, the utilization of EWMA control charts for Poisson observations was investigated, with a focus on process improvement and monitoring. The study covered a number of chapters, including an introduction to Statistical Quality Control and control charts, a review of control charts for Poisson data, and especially for the mean in Poisson processes, the incorporation of time-varying sample sizes, an examination of the Conway-Maxwell-Poisson distribution and a practical application of some of the control charts that were introduced.

First of all, control charts designed for Poisson data provide a useful way for maintaining focused on processes that are described by count or occurrence data. Statisticians are able to precisely watch and manage Poisson processes owing to the unique features of these control charts, such as accounting for the discrete and non-negative nature of observations and assuming independence between occurrences.

Secondly, the ability to monitor the process is improved by combining Poisson data with EWMA control charts. Using exponentially weighted moving averages increases sensitivity and reactivity to changes in the process mean by enabling the detection of tiny shifts and early warning indicators of deterioration. For practitioners looking to quickly identify and correct aberrations in Poisson processes, this integration offers a useful tool.

Additionally, the analysis of time-varying sample sizes in EWMA control charts has brought attention to how crucial adaptability is for tracking Poisson observations. The performance of charts can be improved and process sensitivity can be increased by dynamically modifying sample sizes based on process conditions and performance.

Furthermore, the understanding of additional modeling strategies for Poisson observations has also grown as a result of research into the Conway-Maxwell-Poisson distribution. The study of this distribution's characteristics and its possible use in control charts has revealed new directions for investigation and research.

Lastly, three control charts, introduced in Chapter 2, PEWMA (Poisson Exponentially Weighted Moving Average), PDEWMA (Poisson Double Exponentially Weighted Moving Average), and PTEWMA (Poisson Triple Exponentially Weighted Moving Average), were the subject of a comparison study and performance evaluation in this study. Finding the control chart that would make it possible to spot process changes the quickest was the goal. Notably, the results showed that PTEWMA performed better in detecting negative shifts than the other control charts, proving its usefulness in detecting declines in process performance. However, careful examination of the mean, the size of the shift, and the weighting parameter is crucial when it comes to spotting positive improvements. On the basis of these factors, thoughtful judgments

https://doi.org/10.26219/heal.aueb.6224

may be made regarding the best control chart to use for quickly identifying positive modifications. Organizations can improve their capacity to successfully monitor and improve process performance by carefully evaluating these factors.

Although this thesis has provided insights into EWMA control charts for Poisson observations, there are still a number of areas that might use more investigation.

The application of control charts to additional categories of count data distributions is one promising subject for future research. Despite the fact that the Poisson distribution is frequently used in quality control applications, there are some situations in which zero-inflated models or other alternative count distributions may offer more accurate depictions of the data. The applicability and efficiency of control charting in a wider range of circumstances may be improved by investigating the adaption of EWMA control charts to these distributions.

The practical application discussed in this thesis also provides a framework for additional case studies and empirical research. The usefulness and application of the suggested control charts could be further understood by conducting experiments and validations in various business environments and contexts, as well as by identifying any obstacles and constraints that need to be overcome.

In conclusion, researchers can expand the use of control charting approaches and boost their efficiency in a larger variety of settings by continuing to investigate alternative distributions, such as the zero-inflated models. The proposed control charts will be further validated and improved by conducting additional case studies and empirical investigations across various industry settings and contexts and by broadening the research's focus to include other quality control elements, we will be able to gain a more complete understanding of process performance. This will help reserachers' progress in the discipline of Statistical Quality Control while creating a new way for innovative ideas and developments.

https://doi.org/10.26219/heal.aueb.6224

List of Abbreviations

Abbreviation	Definition
AATS	Adjusted Average Time to Signal
AEQL	Average Extra Quadratic Loss
ARARL	Average Ratio of ARL
ARL	Average Run Length
ASS	Average Sample Size
ATS	Average Time to Signal
CEWMA	Ceil Exponentially Weighted Moving Average
CMP	Conway-Maxwell-Poisson
CMP-DEWMA	Double EWMA for COM-Poisson data
COM-Poisson	Conway-Maxwell-Poisson
CUSUM	Cumulative Sum Control Chart
DEWMA	Double Exponentially Weighted Moving Average
EWMA	Exponentially Weighted Moving Average
EWMAa1	Exponentially Weighted Moving Average using (4.7) equation
EWMAa2	Exponentially Weighted Moving Average using (4.8) equation
EWMAe	Exponentially Weighted Moving Average using (4.6) equation
EWMAG	EWMA when RL follows Geometric Distribution
EWMA-M	modified EWMA method
FEWMA	Floor Exponentially Weighted Moving Average
FIR	Fast Initial Response
FSI	Fixed Sampling Interval
HEWMA	Hybrid EWMA
GEWMA	Generalized Exponentially Weighted Moving Average

IC	In Control
LCL	Lower Control Limit
LRT	Likelihood Ratio Test
MDRL	Median Run Length
MDS	Multiple Dependent Sampling
MWLE	Maximum Weighted Likelihood Estimator
OC	Out Of Control
PCI	Performance Comparison Index
PDEWMA	Poisson Double Exponentially Weighted Moving Average
PEWMA	Poisson Exponentially Weighted Moving Average
PTEWMA	Poisson Triple Exponentially Weighted Moving Average
REWMA	Round Exponentially Weighted Moving Average
RL	Run Length
RPEWMA	Poisson Exponentially Weighted Moving Average using Ranked Set Sampling
RR	Run Rules
RSS	Ranked Set Sampling
RSS CS PEWMA	Combined Shewhart and Poisson Exponentially Weighted Moving Average using Ranked Set Sampling
SDRL	Standard Deviation of the Run Length
SQC	Statistical Quality Control
SRS	Simple Random Sampling
TEWMA	Triple Exponentially Weighted Moving Average
UCL	Upper Control Limit
VSI	Variable Sampling Interval
WEWMA	WLRT-based EWMA
WL	Warning Limit
WLRT	Weighted Likelihood Ratio Test

https://doi.org/10.26219/heal.aueb.6224

References

Abbas, N., 2012. Memory-type control charts in statistical process control. Thesis (PhD). Universiteit van Amsterdam

Abujiya, M.R., 2017a. Monitoring Poisson Observations Using Combined Applications of Shewhart and EWMA Charts, In: 13th IMT-GT International Conference on Mathematics, Statistics and their Applications 2017, 4–7 December 2017,Malaysia. United States of America: AIP Conference Proceedings 1905(1), pp. 050001-1 – 050001-6

Abujiya, M.R., Farouk, A.U., Lee, M.H., Mohamad I., 2013. On the sensitivity of Poisson EWMA control chart. International Journal of Humanities and Management Sciences, 1(1) pp.18-22

Abujiya, M.R., Abbasi, S.A., Riaz, M., 2016. A New EWMA Control Chart for Monitoring Poisson Observations. Quality and Reliability Engineering International, 32(8), pp. 3023-3033

Adeoti, O. A., Malela-Majika, J.-C., 2019. Double exponentially weighted moving average control chart with supplementary runs-rules. Quality Technology and Quantitative Management, 17(2), pp. 149-172

Alevizakos, V., Koukouvinos, C., 2019. A double exponentially weighted moving average control chart for monitoring COM-Poisson attributes. Quality and Reliability Engineering International, 35, pp. 2130–2151

Alevizakos, V., Chatterjee, K., Koukouvinos, C., 2021. The triple exponentially weighted moving average control chart. Quality Technology & Quantitative Management, 18(3), pp.326-354

Alevizakos, V., Chatterjee, K., Koukouvinos, C., 2022. The triple exponentially weighted moving average control chart for monitoring Poisson processes. Quality and Reliability Engineering International, 38(1), pp. 532-549

Aslam, M., Ahmad, L., Jun, C.H., 2014. A multiple dependent state control chart based on double control limit. Research Journal of Applied Sciences, Engineering and Technology, 7(21), pp. 4490–4493

Aslam, M., Ahmad, L., Jun, C.H., Arif, O.H., 2016. A control chart for COM-Poisson distribution using multiple dependent state sampling. Quality and Reliability Engineering International, 32, pp. 2803–2812

 https://doi.org/10.26219/heal.aueb.6224

Aslam, M., Azam, M., Jun, C.H., 2016. A control chart for COM-Poisson distribution using resampling and exponentially weighted moving average. Quality and Reliability Engineering International, 32, pp. 727–735

Aslam, M., Khan, N., Jun, C.H., 2018. A hybrid exponentially weighted moving average chart for COM-Poisson distribution. Transactions of the Institute of Measurement and Control, 40, pp. 456–461

Aslam, M., Saghir, A., Ahmad, L., Jun, C.H., Hussain, J., 2017. A control chart for COM-Poisson distribution using a modified EWMA statistic. Journal of Statistical Computation and Simulation, 87, pp. 3491–3502

Borror, C.M., Champ, C.W., Rigdon, S.E., 1998. Poisson EWMA control charts. Journal of Quality Technology, 30(4), pp. 352-361

Conway, .RW., Maxwell, W.L. ,1962. A queuing model with state dependent service rates. Journal of Industrial Engineering, 12, pp. 132–136

Dong, Y., Hedayat, A.S., Sinha, B.K., 2008. Surveillance strategies for detecting changepoint in incidence rate based on exponentially weighted moving average methods. Journal of the American Statistical Association, 103(482), pp. 843-853

Epprecht, E.K., Simões, B.F.T., Mendes, F.C.T., 2009. A variable sampling interval EWMA chart for attributes. International Journal of Advanced Manufacturing Technology, 49(1-4), pp. 281-292

Gan, F.F., 1990a. Monitoring poisson observations using modified exponentially weighted moving average control charts. Communications in Statistics - Simulation and Computation, 19(1), pp. 103-124

Haq, A., 2013. A New Hybrid Exponentially Weighted Moving Average Control Chart for Monitoring Process Mean. Quality and Reliability Engineering International, 29(7), pp. 1015–1025

Hawkins, D. M., Olwell D. H., 1998. Cumulative Sum Charts and Charting for Quality Improvement, New York: Springer-Verlag

Khan, N., Aslam, M., Jun, C.-H., 2016. Design of a Control Chart Using a Modified EWMA Statistic. Quality and Reliability Engineering International, 33(5), pp. 1095–1104

Mei, Y., Han, S. W., and Tsui, K.-L. ,2011. Early Detecting of a Change in Poisson Rate After Accounting for Population Size Effects. Statistica Sinica, 21, pp. 597–624

Montgomery, D.C., 2009. Introduction to Statistical Control 6th ed. United States of America: John Wiley & Sons, Inc

Page, E.S., 1961 Cumulative Sum Charts, Technometrics, 3(1), pp. 1-9

https://doi.org/10.26219/heal.aueb.6224

Roberts, S.W., 1959. Control chart tests based on geometric moving averages. Technometrics, 1(3), pp. 239-250

Ryan, A.G., Woodall, W.H., 2010. Control charts for poisson count data with varying sample sizes. Journal of Quality Technology, 42(3), pp. 260-275

Saghir, A., Lin, Z., 2014. A flexible and generalized exponentially weighted moving average control chart for count data. Qual Quality and Reliability Engineering International, 30, pp. 1427–1443

Saghir, A., Lin, Z., Abbasi, S. A., Ahmad, S., 2012. The Use of Probability Limits of COM-Poisson Charts and their Applications. Quality and Reliability Engineering International, 29(5), pp. 759–770

Sellers, K. F., 2011. A generalized statistical control chart for over- or under-dispersed data. Quality and Reliability Engineering International, 28(1), pp. 59–65

Shamma, S.E., Amin, R.W., Shamma, A.K., 1991. A double exponentially weighted moving average control procedure with variable sampling intervals. Communication in Statistic - Simulation and Computation, 20(2-3), pp. 511-528

Shamma, S.E., Shamma, A.K., 1992. Development and evaluation of control charts using double exponentially weighted moving averages. International Journal of Quality & Reliability Management, 9, pp. 18-25

Shen, X., Zou, C., Jiang, W., Tsung, F., 2013. Monitoring poisson count data with probability control limits when sample sizes are time varying. Naval Research Logistics, 60(8), pp. 625-636

Sherman R.-E., 1965. Design and evaluation of a repetitive group sampling plan. Technometrics , 7(1), pp. 11–21

Shmueli, G., Minka, T.P., Kadane, J.B., Borle, S., Boatwright, P., 2005. A useful distribution for fitting discrete data: Revival of the Conway–Maxwell–Poisson distribution. Journal of the Royal Statistical Society: Series C (Applied Statistics), 54(1), pp. 127–142

Shu, L., Jiang, W., & Wu, Z., 2012. Exponentially weighted moving average control charts for monitoring increases in Poisson rate. IIE Transactions, 44(9), pp. 711–723

Steiner, S. H., 199. EWMA Control Charts with Time-Varying Control Limits and Fast Initial Response. Journal of Quality Technology, 31(1), pp. 75–86

Testik, M.C., McCullough, B.D., Borror, C.M., 2006.The effect of estimated parameters on Poisson EWMA control charts. Quality Technology and Quantitative Management, 3(4), pp. 513–527

https://doi.org/10.26219/heal.aueb.6224

Wortham, A. W., Baker, R. C, 1976. Multiple deferred state sampling inspection. International Journal of Production Research, 14(6), pp. 719–731

Zamanzade, E., Mahdizadeh, M., 2020. Using ranked set sampling with extreme ranks in estimating the population proportion. Statistical Methods in Medical Research, 29(1), pp. 165-177

Zhang, L., Govindaraju, K., Lai, C.D., Bebbington, M.S., 2003. Poisson DEWMA Control Chart. Communications in Statistics Part B:Simulation and Computation, 32(4), pp.1265-1283

Zhou, Q., Zou, C., Wang, Z., Jiang, W., 2012. Likelihood-based EWMA charts for monitoring poisson count data with time-varying sample sizes. Journal of the American Statistical Association, 107(499), pp. 1049-1062